ORIGINAL ARTICLE

Impaired cell adhesion, apoptosis, and signaling in WASP gene-disrupted Nalm-6 pre-B cells and recovery of cell adhesion using a transducible form of WASp

Rikiya Sato · Susumu Iizumi · Eun-Sung Kim ·
Fumiko Honda · Sang-Kyou Lee · Noritaka Adachi ·
Hideki Koyama · Shuki Mizutani · Tomohiro Morio

Abstract Wiskott–Aldrich syndrome (WAS) is an X-linked immunodeficiency disease affecting cell morphology and signal transduction in hematopoietic cells. The function of Wiskott–Aldrich syndrome protein (WASp) and its partners in protein interaction have been studied intensively in mice; however, detailed biochemical characterization of its signal transduction and assessment of its functional consequence in human WASp-deficient lymphocytes remain difficult. In this study, we generated Nalm-6 cells in which the WAS protein gene (WASP) was disrupted by homologous recombination-based gene targeting and a cell-permeable form of recombinant WASp for functional study. The WASP$^{-/-}$ cells showed impaired adhesive capacity and polarization to plate-bound anti-CD47 mAb, anti-CD9 mAb, or to fibronectin. The defective morphological changes were accompanied by impaired intracellular signaling. In addition, the WASp-deficient cells displayed augmented apoptosis induced by CD24 cross-linking. A recombinant fusion protein composed of Hph-1 cell-permeable peptide and WASp prepared in *Escherichia coli*. Hph-1-WASp was efficiently transduced and expressed in WASP$^{-/-}$ Nalm-6 cells in a dose-dependent manner. The wild-type WASp, but not the mutant restored adhesion capacity, spreading morphology, and cytoskeletal reorganization. Additionally, the recombinant protein was successfully transduced into normal lymphocytes. These findings suggest that gene-disrupted model cell lines and cell-permeable recombinant proteins may serve as important tools for the detailed analysis of intracellular molecules involved in PID.

Keywords Wiskott–Aldrich syndrome · Gene targeting · Protein transduction domain · Gene therapy

R. Sato · F. Honda · S. Mizutani · T. Morio (✉)
Department of Pediatrics and Developmental Biology,
Tokyo Medical and Dental University Graduate School
of Medicine, 1-5-45 Yushima, Bunkyo-ku,
Tokyo 113-8519, Japan
e-mail: tmorio.ped@tmd.ac.jp

S. Iizumi · N. Adachi · H. Koyama
Kihara Institute for Biological Research, Graduate School
of Integrated Science, Yokohama City University,
641-12 Maioka-cho, Totsuka-ku, Yokohama 224-0813, Japan

E.-S. Kim · S.-K. Lee
Department of Biotechnology, College of Life Science
and Biotechnology, National Creative Research Initiatives
Center For Inflammatory Response Modulation,
Yonsei University, 134 ShinChon-dong, SoDaeMun-gu,
Seoul 120-749, South Korea

Introduction

Wiskott–Aldrich syndrome (WAS) is an X-linked immunodeficiency disease characterized by thrombocytopenia with small platelet volume, eczema, and recurrent infections [1, 2]. WAS is caused by a variety of mutations in the WAS protein (WASp) gene (*WASP*) which is expressed in cells of hematopoietic origin [3–5]. WASp is a member of a distinct family of proteins that participates in transduction of signals from the cell surface to the actin cytoskeleton. Defect related to WASp lead to faulty cell migration, proliferation, and survival [6–9].

The structure and functional biochemistry of WASp has been extensively studied. WASp has several principal domains that regulate its function and subcellular localization. These include a WH1 domain, a basic region, a GTPase-binding domain, a proline-rich region, a verprolin homology domain, a central domain, and an acidic domain. The WH1 domain of WASp interacts with WIP, a protein

Ⓓ Springer

that stabilizes WASp-regulated actin filaments, and is important for filopodium formation [10, 11]. The proline-rich region of WASp is required for optimal actin-polymerization activity. The region provides binding sites for SH3 domain containing proteins, including adaptor proteins (CIP4, Nck, Grb2, PSTPIP, and intersectin-2) and tyrosine kinases (Fyn, Lyn, Hck, and Btk), which may phosphorylate and activate WASp [6–9, 12–15]. One of the key mechanisms of WASp activation is through specific interaction of a Cdc42- and Rac-interactive binding domain of WASp with GTP-bound Cdc42. Cdc42 regulates the formation of filopodium formation and cell–substrate adhesions, and controls cell polarity and motility [9, 16, 17].

Functional and biochemical analysis of WASp-deficient immune cells has been explored using splenic cells of *Wasp*-disrupted mice, an Epstein–Barr virus-transformed lymphoblastoid cell line (EBV-LCL), human T-cell leukemia virus type 1 (HTLV-1)-transformed T lymphocytes, and peripheral blood lymphocytes from human WAS patients. $WASP^{-/-}$ T cells fail to reorganize actin filaments in response to T-cell receptor engagement, and are defective in forming cell-activating immunological synapses. T-cell signaling is impaired in WASp-deficient cells, leading to incomplete cell activation and abnormal proliferation. T cells from patients with WAS also display aberrant expression of surface antigens, including downregulation of sialylated surface proteins such as CD43, CDw75, and CD76 surface determinants generated by β-galactoside α-2,6 sialyl transferase [18]. Although previous data show abnormal cell morphology as well as impaired receptor capping and surface marker expression in WASp-deficient B cells [19], a detailed biochemical study of human B cells has been difficult and yet to be explored [19–26].

In this study, we examined the functional and biochemical defects of human B cells by generating a WASp-deficient B-cell line: *WASP* gene was disrupted in a human pre-B-cell line, Nalm-6, by homologous recombination for in-depth analysis of morphological change and actin reorganization induced by signal through various receptors. To generate the model cell line, we used a simplified vector construction system and a high-efficiency gene-targeting method, which enables rapid disruption of any locus of the human genome in a short period of time [27, 28].

Practical gene/protein correction systems should permit detailed biochemical and functional studies of a particular molecule in immune cells involved in human primary immunodeficiency disease. One frequently used method is a retrovirus-mediated gene transduction system; however, this technique is still labor intensive and has difficulties related to controllable protein expression. A minimally toxic and efficient intracellular WASp delivery system would allow detailed functional studies of cell lines as

well as primary cells. In this study, we employed protein delivery through a novel cell-permeable protein transduction domain (PTD) for functional reconstitution assay in the *WASP*-disrupted cells. The peptide is from the human transcription factor Hph-1 [29], and has transduction efficiency comparable to TAT (the protein transduction domain of transactivating transcription polypeptide), minimal toxicity, and reasonable stability in vitro and in vivo.

We here report our findings with regard to the cell adhesion and protrusion induced by CD47 engagement, CD9 crosslinking, or by fibronectin, and cell apoptosis induced by CD24 crosslinking in the WASp-deficient cells. We studied differences in tyrosine phosphorylation of protein tyrosine kinases (PTKs) elicited by the engagement of CD47 and CD9 between wild-type (wt) and WASp-deficient Nalm-6 cells. A fusion protein composed of Hph-1 and full-length WASp, but not mutant recombinant WASp, complemented cellular dysfunction caused by the *WASP* mutation.

Materials and methods

Construction of targeting vectors

Construction of targeting vectors was performed as described previously [28]. Briefly, 1.8- and 2.3-kb genomic fragments were obtained by PCR with Platinum PCR SuperMix High Fidelity (Invitrogen Japan, Tokyo, Japan) using genomic DNA from healthy donors as a template, verified by DNA sequencing, and were used as 5′ and 3′ arms, respectively, in a pDONR vector. The primer sequences used for the 5′ arm were 5′-GGGGACAACTTT GTATAGAAAAGTTGGCCTCGCCAGAGAAGACAAG-3′ and 5′-GGGGACTGCTTTTTTGTACAAACTTGAGTAC AGCTCCTGTTCCCAGA-3′, and those for the 3′ arm were 5′-GGGGACAGCTTTCTTGTACAAAGTGGCCAC TCCCTCCTGCTCTG-3′ and 5′-GGGGACAACTTTGT ATAATAAAGTTGTGAGTGTGAGGACCAGGCAG-3′. Using MultiSite Gateway® Technology (Invitrogen Japan), a floxed Puro^r gene was inserted between the 5′ and 3′ arms on a plasmid carrying a diphtheria toxin A gene.

Cell line and transfection

EBV-LCL was established from healthy donors and from patients with WAS. Studies using the patients' cell lines were approved by the institutional ethical committee. Human Nalm-6 cells of pre-B-cell origin with an XY karyotype were cultured in ES medium (Nissui Seiyaku, Tokyo, Japan) supplemented with 10% fetal calf serum (FCS) and 50 μM 2-mercaptoethanol. DNA transfection

was carried out as described previously [27, 28]. Briefly, 4×10^6 cells were electroporated with 1.65 μg of targeting vector linearized with *PmeI* in a 40-μL chamber of Electro Gene Transfer Equipment (GTE-1; Shimadzu, Kyoto, Japan). After a 22-h incubation, the cells were incubated for an additional 2 weeks at 37°C in 0.15% agarose medium containing 0.5 μg/mL puromycin. Genomic DNA was isolated from drug-resistant colonies and subjected to PCR analysis. The cell lysates were analyzed by anti-WASp immunoblot.

PCR analysis of drug-resistant clones

Genomic DNA isolated from puromycin-resistant colonies was screened by PCR using a primer from a promoter region of the WASP gene (5'-TTTACTGTAGTAACCCTT CCGGACT-3') and a primer (5'-AATAATGGTTTCTTA GACGTGCG-3') located between the attL1 and lox-P sequences of Puro^r.

Cell aggregation assay

For assessing cell aggregation through CD9 engagement, cells were incubated at 3×10^5/mL with anti-CD9 mAb (ALB6) at 0.5 μg/mL in 24-well flat-bottomed plates (BD Falcon) for 48 h, and inspected under a microscope.

Cell adhesion and polarization assay

For this procedure, 96-well flat-bottomed plates were pre-coated with anti-CD47 mAb or with anti-CD9 mAb at 10 μg/mL in 100 μL of 0.1 M NaHCO3 buffer (pH 9) overnight at 4°C, and then washed and blocked with 5% FCS/PBS. Wt or WASp-deficient Nalm-6 cells were seeded in the plates at 5×10^4/100 μL. After a 1-h incubation, the number of adherent cells with a spreading morphology was counted in the indicated area under phase-contrast microscopy. At least 750 cells in eight wells were counted blindly, and the proportion of polarized cells calculated as follows:

$$\% \text{polarized cells} = (\text{polarized cell number}/\text{total cell number}) \times 100$$

The cells were then washed with PBS, and firmly attached cells were counted with phase-contrast microscopy. Adhesion to fibronectin-coated 96-well flat-bottomed plates (BD Biosciences, Bedford, MA, USA) was assessed by incubating 5×10^4 cells in the plates for 2 h and then inspecting for adherent cells with phase-contrast microscopy. The cells were also stained with Rhodamine-conjugated phalloidin (Sigma, St. Louis, MO, USA) and were inspected under a fluorescence microscope (Zeiss).

Stimulation of Nalm-6 cells for signal transduction assay

Wt or WASp-deficient Nalm-6 cells in Hanks' balanced salt solution (HBSS) at 2×10^6/200 μL were stimulated with 2 μg of anti-CD9 mAb (ALB6) for pre-established times. For stimulation with CD47, the cells were put into anti-CD47 mAb-precoated 24-well plates at 1×10^6/400 μL, incubated at 20°C for 2 min, and then stimulated by incubating the plate at 37°C for pre-established times. The reaction was quenched by adding 600 μL of ice-cold HBSS and subsequently centrifuging the collected cells.

Induction of apoptosis by crosslinking of CD24 and detection of apoptosis by flow cytometry

Wt or WASp-deficient Nalm-6 cells were stimulated with anti-CD24 mAb (5 μg/ml) in the presence of rabbit secondary anti-mouse IgG antibody (10 μg/ml) for indicated time period. To detect apoptosis induced by crosslinking of CD24, the cells were stained with FITC-labeled Annexin V (Roche Applied Science, Mannheim, Germany) and 7-AAD (Sigma, St. Louis, MO, USA). The cells were then analyzed by flow cytometry according to the manufacturer's instruction.

Western blot

The cell lysates were prepared by incubating cells in a lysis buffer [1% NP40, 20 mM Hepes (pH 7.55), 150 mM NaCl, 50 mM NaF, 1 mM Na3VO4] supplemented with protease inhibitor cocktail (Sigma, St. Louis, MO, USA) for 30 min on ice. The lysates were centrifuged at 14,000 rpm at 4°C for 30 min and stored at −80°C until further analysis.

Western blot analysis with anti-phosphotyrosine antibody (4G10), anti-CD43 (L10), or anti-WASp antibody (5A5) was carried out as previously described [4, 44]. Rabbit polyclonal antibody to Btk phosphorylated at Tyr223, Syk phosphorylated Tyr525/526, Src phosphorylated Tyr416, and PLCγ1 phosphorylated at Y783 were sourced from Cell Signaling Technology. Rabbit polyclonal antibody to Lyn phosphorylated at Tyr396 was obtained from Abcam. An equal amount of loading was confirmed by staining the transferred blot with Ponceau S or by probing with anti-β-actin antibody.

Immunoprecipitation

Immunoprecipitation was carried out as previously described [4, 44]. Briefly, the cell lysates were incubated with protein G Sepharose beads (GE Healthcare Life Sciences) preadsorbed with normal rabbit serum/normal mouse serum overnight. The precleared cell lysates were

immunoprecipitated sequentially with protein G beads prereacted with anti-Syk (Santa Cruz Biotechnology, Santa Cruz, CA, USA), anti-Btk (a gift from Dr. Hirokazu Kanegane), anti-PLC-γ1 (Cell Signaling Technology), and anti-Lyn (Santa Cruz Biotechnology) for 1 h. The immunoprecipitates were washed and resolved with 9% sodium dodecyl sulfate polyacrylamide gel electrophoresis (SDS-PAGE) and then immunoblotted with 4G10.

MAbs and flow cytometric analysis

Antibodies used were fluorescein isothiocyanate (FITC)-conjugated mAbs to MsIgG, MsIgM, CD10, CD19, CD20, HLA-DR (BD Pharmingen), CD9, CD29, CD49d (Immunotech, Marseille), CD49e (Beckman Coulter Japan, Tokyo), CD43 (eBiosciences, San Diego, CA, USA), MsIgG2 (Southern Biotech, Birmingham, AL, USA), Annexin V (Roche), PE-conjugated mAbs to CD18, CD38, CD40 (Immunotech), MsIgG1, CD20, CD54 (BD Pharmingen), biotin-labeled mAb to phosphotyrosine (4G10) (Upstate); and unlabeled mAb to CD24, CD37, CD47, WASp (5A5) (BD Pharmingen), CD43, CD81, BAFF-R (eBiosciences), CD81(Santa Cruz Biotechnology), and β-actin (Sigma). Isotype-matched controls (FITC-MsIgG1, FITC-MsIgG2, FITC-MsIgM, and PE-MsIgG1) were procured from BD Pharmingen. Anti-CD24 mAb (L30), anti-CD40 mAb (G28-5) and CDw76 mAb (HD66) were provided by Dr. Kiyokawa, Dr. Ed Clark and Dr. Gerhard Moldenhauer, respectively.

The surface phenotypes of cells were examined by flow cytometry, as previously described [45]. At least 10,000 events were counted and analyzed for each staining.

Generation of Hph-1-WASp and induction into cells

Hph-1-wt *WASP* was generated by amplifying *WASP* cDNA fragments with the following primers: 5′-GCCTCG CCAGAGAAGACAAG-3′ and 5′-TGAGTGTGAGGACC AGGCAG-3′ from cDNA prepared from healthy controls. Hph-1-*WASP* mutant A and -*WASP* mutant E constructs were generated by amplifying *WASP* cDNA fragments from cDNAs of the patients, which harbor stop codon, with the same primers used for wt constructs, verifying the DNA sequences, then cloning into Hph-1-wt *WASP* vector. After verification by DNA sequencing, the fragment was ligated into *Eco*RI-cleaved and *Hin*dIII-cleaved sites of pRSET_B vector which contained 6× His sites for protein purification and 2× Hph-1 sequences for efficient protein transduction.

Protein induction was carried out as previously described [29]. Briefly, the expression of Hph-1-WASp was induced without using IPTG, in Rosetta™2(DE3)pLysS bacteria strain (Novagen) transformed with each DNA construct overnight in LB medium with the addition of

glucose, lactose, glycerol, phosphates and hydrosulfates. It was then sonicated in a lysis buffer [10 mM imidazole, 20 mM Tris–HCl (pH 8.0), and 500 mM NaCl]. The lysates were clarified by centrifugation and loaded on His-Trap chelating columns (QIAGEN). Bound proteins were washed and eluted with 300 mM imidazole. Eluted proteins were desalted using PD-10 Sephadex™ G-25 columns, concentrated using Microcon filters (Amicon), and frozen at −80°C until used.

The cells were incubated with 1, 2, 5, or 10 μM of Hph-1-WASp or with control Hph-1-Gal4 protein at 10^6 cells/mL for 60 min, washed, and then subjected to further analysis. A total of 70 μg of the recombinant protein was used for transduction at 1 μM.

Results

### Establishment of *WASP* gene-disrupted Nalm-6 pre-B cells

To disrupt the *WASP* gene in the Nalm-6 human pre-B-cell line, we constructed a targeting vector, pWASP-puro, carrying a puromycin-resistance gene flanked by the 1.8- and 2.3-kb *WASP* sequences. A diphtheria toxin A gene was added to the construct for selection against random integrants. Genes of 1.8- and 2.3-kb *WASP* sequences encompass exons 1–3 and mid-exons 10–12, respectively (Fig. 1a).

The targeting vector was linearized with *Pme*I and electroporated into Nalm-6 cells. A total of 288 puromycin-resistant clones were isolated and subjected to polymerase chain reaction (PCR) analysis using a primer from the 5′UTR region and a primer from the puromycin cassette. Three clones (2D2, 4F2, and 6E3) exhibited band patterns indicative of the recombination (Fig. 1b). To examine whether the precise recombination event occurred in these clones, Western blot analysis was carried out with 5A5 anti-WASp antibody which recognizes an epitope encompassing amino acids 146–265. Expression of WASp was absent in all selected clones (Fig. 1c).

WASp-deficient Nalm-6 pre-B cells are defective in cell adhesion and polarization induced by anti-CD47, anti-CD9, and fibronectin

WASp-deficient B cells in mice and human fail to display cytoskeletal reorganization and are unable to alter cell morphology upon stimulation [19]. We investigated whether the *WASP* gene-disrupted Nalm-6 cells similarly show defective cell aggregation, adhesion, and polarization on exposure to various stimuli.

We first examined the capacity of cell morphological changes induced by the engagement of CD47, an integrin-
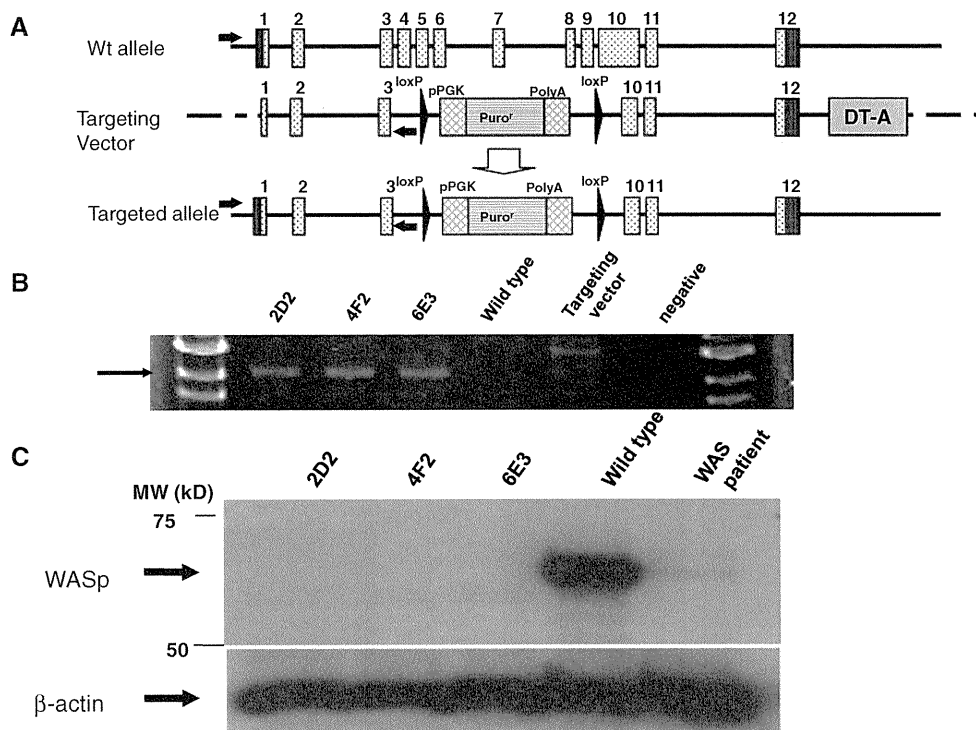
Fig. 1 Targeted disruption of the human *WASP* gene in Nalm-6 cell line. **a** Scheme of *WASP* gene targeting: The p*WASP*-puro targeting vector is designed to delete a region encompassing exon 4 to mid-exon 10 by the puromycin-resistant gene. **b** PCR analysis of drug-resistant clones: PCR analysis with primers indicated by *arrows* in **a** was carried out in 288 puromycin drug-resistant clones, among which 2D2, 4F2, and 6E3 clones were positive for the 5' arm of the

WASP gene and the puromycin-resistant gene. **c** Western blot analysis of the PCR-confirmed gene-disrupted clones: The 2D2, 4F2, and 6E3 clones were subjected to anti-WASp immunoblotting. EBV-LCL from a normal subject and a patient with WAS served as positive and negative controls, respectively. Positions of WASp and *β*-actin (loading control) are indicated by *arrows*
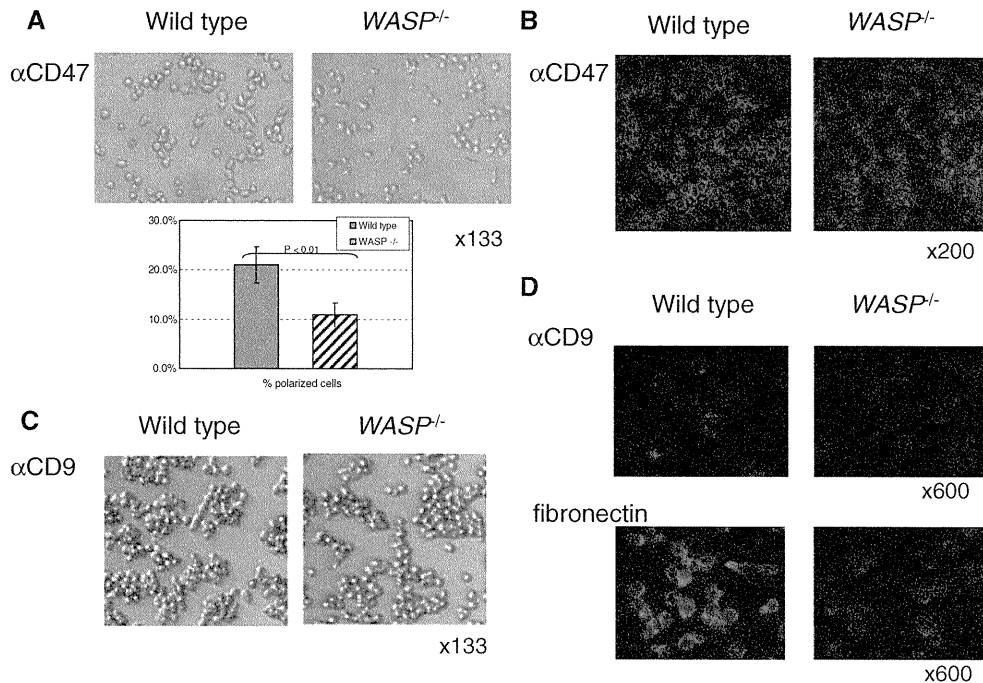
associated protein that serves as a ligand for VLA-3, VLA-4, thrombospondin-1, and Src homology domain-2-containing protein tyrosine phosphatase substrate 1 (SHPS-1) [30, 31]. Wt and *WASP*$^{-/-}$ Nalm-6 cells did not bind to an uncoated flask (data not shown). The proportion of adherent cells with protrusion was estimated by counting a total of at least 700 cells. Combined results from three independent experiments show 21.3% of wild-type (wt) Nalm-6 cells firmly adhered to anti-CD47-coated plates with a polarized morphology within 1 h (Fig. 2a, left and bottom panels). In contrast, 11.0% of 2D2 cells demonstrated adhesion with a spreading morphology at 1 h following stimulation with plate-bound anti-CD47, which was significantly less than that observed in wt cells ($p < 0.01$) (Fig. 2a, right and bottom panels). To check the cytoskeletal morphology induced by CD47 engagement more in detail, F-actin fibers were visualized with Rhodamine-conjugated phalloidin and a fluorescence microscope. Accumulation of F-actin fibers on the contact site of adjacent cells was observed in wt cells, whereas F-actin localization was diffuse in WASp-deficient cells (Fig. 2b).

We next examined CD9-mediated cell morphological changes in *WASP*$^{-/-}$ cells. CD9 is a member of trans-membrane 4 superfamily involved in cell-to-cell interaction and motility, and serves as a ligand for PSG17 [32]. Although cell aggregation induced by soluble anti-CD9 was not affected (Fig. 2c), morphological change and actin reorganization induced by plate-bound anti-CD9 was severely impaired in the absence of WASp (Fig. 2d, upper panel). Actin reorganization elicited by fibronectin was also virtually absent in 2D2 cells (Fig. 2d, lower panel). Collectively, these results indicate that WASp-deficient Nalm-6 cells are grossly impaired in cytoskeletal reorganization induced by different ligands.

Impaired signal transduction through CD47 in the absence of WASp

We next sought to explore the potential signaling defects which led to the defective morphological changes and cell adhesion in WASP$^{-/-}$ cells.

Nalm-6 and 2D2 cells were stimulated by anti-CD47 mAb for indicated time period; and tyrosine phosphorylation of

A Wild type   WASP⁻/⁻   **B**   Wild type   WASP⁻/⁻

αCD47   αCD47

                                                                        x200

              x133   **D**   Wild type   WASP⁻/⁻

C   Wild type   WASP⁻/⁻   αCD9

αCD9

                                                                        x600
                                        fibronectin

              x133

                                                                        x600

Fig. 2 Cytoskeletal reorganization induced by stimulation with anti-CD47, anti-CD9, and fibronectin was defective in WASp-deficient 2D2 cells. **a** Defective cell adhesion with a protrusion morphology was detected in 2D2 cells cultured in anti-CD47 mAb-coated plates. Both wt and WASp-deficient cells were seeded at 5×10^4 cells/ 100 µL in a 96-well flat-bottomed plate precoated with anti-CD47 mAb (8 wells each), incubated for 1 h, and then examined by phase-contrast microscopy. The figure shown is representative of three independent experiments. The percentage of adherent cells with polarization was evaluated by counting at least 750 cells from six wells in each experiment. The experiments were repeated three times, and the mean percentage and SD calculated from the cumulative data are shown in *lower panel*. Each *error bar* indicates SD. **b** Defective

F-actin accumulation on contact sites of neighboring 2D2 cells stimulated with plate-bound anti-CD47 mAb: Wt and 2D2 cells were stained with phalloidin-Rhodamine after stimulation in anti-CD47 mAb-coated plates for 1 h. One representative picture out of four independent experiments was shown. **c** CD9-ligation induced cell aggregation was not affected in WASp-deficient Nalm-6 cells Wt Nalm-6 cells and 2D2 cells were stimulated for 48 h with soluble anti-CD9 mAb, and was observed under phase-contrast microscopy. **d** Defective F-actin accumulation in 2D2 cells stimulated with plate-bound anti-CD9 mAb (*upper panel*) or with fibronectin (*lower panel*). One representative picture from three independent experiments was shown

cellular substrates were monitored by anti-phosphotyrosine (4G10) immunoblot. The stimulation induced rapid and sustained phosphorylation of various protein species in the 35-, 50–53-, 70-, 72-, 80-, and 150-kDa range in wt Nalm-6 cells (Fig. 3a, left panel). In contrast, tyrosine phosphorylation of these cellular substrates upon stimulation was generally decreased and rapidly fell down below the basal level in 2D2 *WASP⁻/⁻* cells (Fig. 3a, right panel).

We next attempted to identify the molecules that were phosphorylated through CD47 signal in Nalm-6 cells, since intracellular targets of the CD47-mediated signal in immune cells remain unknown. We evaluated the potential involvement of the following signaling molecules: Lyn, a 50–53-kDa protein; Syk and Btk, 70–80-kDa proteins, and PLC-γ1, a 150-kDa range molecule. First, wt Nalm-6 cells were stimulated with plate-bound CD47 mAb for 2 and 10 min. The cell lysates were subjected to sequential immunoprecipitation with anti-Syk, anti-Btk, anti-PLC-γ1, and anti-Lyn antisera, and then to an anti-phosphotyrosine blot.

Figure 3b demonstrates that tyrosine phosphorylation of p72 Syk is upregulated following CD47 ligation. We observed >3-fold increase of Syk phosphorylation over base line in three independent experiments. Only modest phosphorylation of Lyn was observed upon CD47 stimulation; and significant changes in Btk or PLC-γ1 were not induced by CD47 engagement (Fig. 3b). We next examined the phosphorylation of Syk, Btk, Lyn, c-Src, and PLC-γ1 using phospho-specific antibodies in wt and *WASP⁻/⁻* Nalm-6 cells. Phosphorylation of Syk, Btk, Lyn, and c-Src at the activation loop tyrosine was not induced by CD47-mediated signal in 2D2 cells (Fig. 3c). Increased phosphorylation of Syk was observed in CD47-stimulated wt Nalm-6 cells, however, unexpectedly; the levels of phosphorylation at positive regulatory tyrosine residues in Btk, Lyn, and c-Src were decreased upon CD47 engagement (Fig. 3c). Phosphorylated PLCγ1 was not detected by phospho-specific Ab (data not shown). These data imply that Syk is activated through CD47 receptor in Nalm-6 pre-B cells.
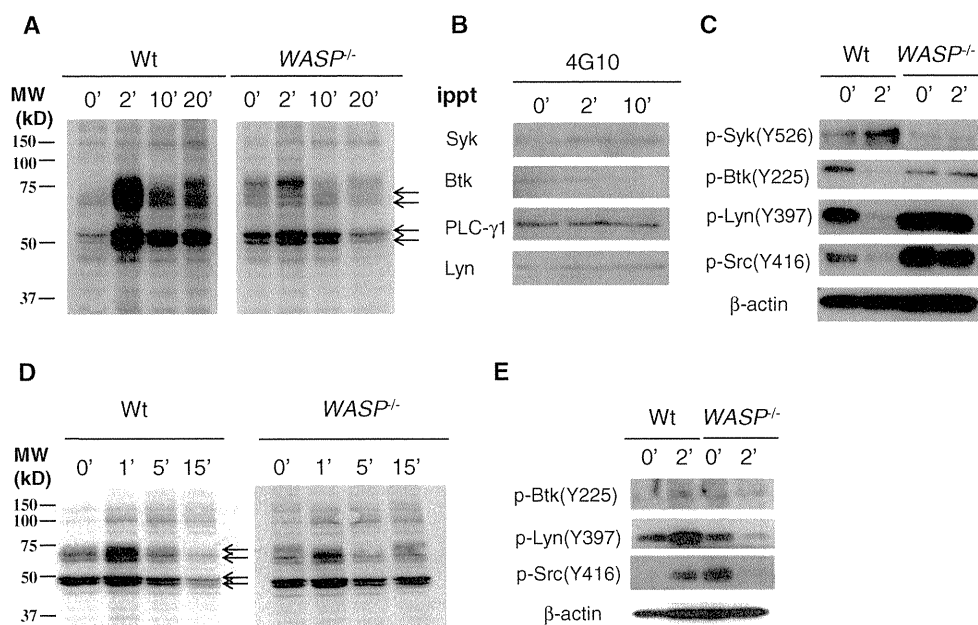
Fig. 3 Signal transduction through the CD47 receptor is affected in WASp$^{-/-}$ cells **a** CD47-mediated signaling is affected in WASp-deficient cells. Wt and WASp$^{-/-}$ cells were plated in anti-CD47-coated wells for 5 min at 4°C and then stimulated for 2, 10, and 20 min at 37°C. The cell lysates were prepared and blotted with anti-phosphotyrosine. One representative 4G10 blot out of four independent experiments is shown. An equal amount of loading in each lane was confirmed by staining with Ponceau S. **b** Syk but not Btk, Lyn or PLC-γ1 is intracellular targets of CD47-signaling in Nalm-6 cells. The cell lysates prepared from wt Nalm-6 cells were sequentially immunoprecipitated with anti-Syk, -Btk, -PLC-γ1, and -Lyn. The precipitates were analyzed by anti-phosphotyrosine blotting. One representative blot out of three independent experiments is shown. **c** CD47-ligation activates Syk in wt Nalm-6 cells but not in 2D2 cells.

Cells were stimulated in plate-bound CD47mAb for 2 min, and the cell lysates were proved with indicated phospho-specific antibody. One out of three independent experiments is shown. β-actin is shown as a loading marker. **d** CD9-mediated signal is similar in 4G10 blot between wt Nalm-6 and WASP$^{-/-}$ cells. A total of 2 × 10^6 cells were stimulated with anti-CD9 mAb at 1 μg/10^6 cells for indicated time periods and lysed. The cell lysates were subjected to anti-phosphotyrosine blotting. Figure shows one representative blot from three independent experiments. **e** CD9-mediated phosphorylation of Btk, Lyn, and c-Src is impaired in WASP$^{-/-}$ cells. Cells were stimulated with anti-CD9 mAb for indicated time and were subjected to Western blot with indicated phospho-specific antibodies. One representative data out of two independent experiments are shown

The observed overall tyrosine phosphorylation pattern was not due to a peculiarity of 2D2 cells because similar results were obtained in 4F2 and 6E3 cells as well (data not shown).

We next examined the effect of WASp deficiency in CD9-mediated signaling. CD9 ligation resulted in a rapid increase in phosphorylation of multiple proteins in the 50–53-, 70-, 72-, and 110-kDa range in wt cells; and kinetics and magnitude of the tyrosine phosphorylation were marginally altered but not significantly different in 2D2 cells (Fig. 3d). Immunoblot with the phospho-specific antibodies on wt Nalm-6 and 2D2 cells showed that Btk, Lyn, and c-Src were phosphorylated in wt Nalm-6 cells upon CD9 engagement, whereas the phosphorylation was down-regulated in WASp-deficient Nalm-6 cells (Fig. 3e).

Although decreased activation of the PTKs upon CD47 engagement in wt Nalm-6 cells warrants further investigation; and the contribution of individual PTK in the process of actin reorganization triggered by CD9 or CD47 signaling in pre-B cells remains to be determined in further

studies, these results indicate that altered intracellular signaling may underline impaired cytoskeletal changes triggered by the engagement of CD9 and CD47 in WASp deficiency.

Apoptosis induced by crosslinking of CD24 is increased in WASP$^{-/-}$ Nalm-6 cells

Abnormal apoptosis is potentially involved in autoimmunity, malignancy, or both in WAS patients [33]. Since apoptosis can be induced in pre-B-cell line via signaling through CD24 [34–36], we examined the apoptotic behavior in the presence or absence of WASp by treating wt Nalm-6 cells or 2D2 cells with anti-CD24 mouse mAb and secondary anti-mouse IgG antibodies. Apoptotic cells were enumerated by Annexin-V positivity detected by a flow cytometry. As shown in Fig. 4a, Annexin-V positive cells were increased in 2D2 cells compared with wt Nalm-6 cells. Combined results from four independent experiments showed that 14.9% of WASP-null Nalm-6 cells underwent apoptosis, whereas

Fig. 4 CD24-induced apoptosis was increased in the absence of WASp. **a** Apoptosis was induced by crosslinking of CD24 in WASp-proficient and -deficient Nalm-6 cells. The cells were then stained with FITC-Annexin V and 7-AAD, and analyzed by a flow cytometry. Annexin V+7-AAD− cells represent the cells in early apoptosis, and Annexin V+7-AAD+ cells represent the cells in late apoptosis. We enumerated Annexin-V positive cells regardless of positivity for 7-AAD. **b** Percentage of cells with apoptosis induced by crosslinking of CD24. Data show a summary from four independent experiments. Mean ± SD is indicated
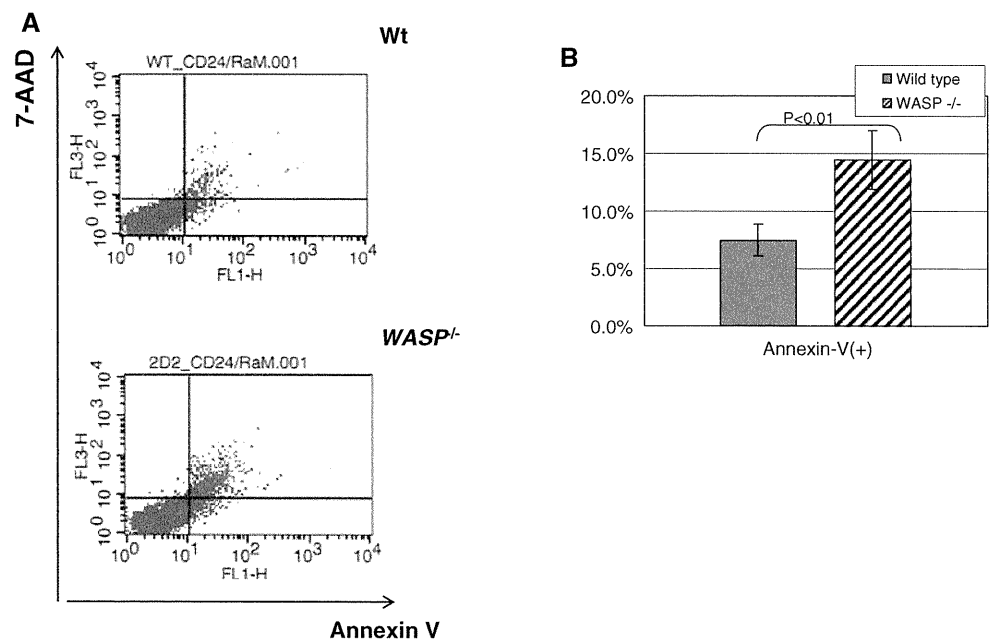
7.4% of wt Nalm-6 cells exhibited apoptosis after 2 h stimulation through CD24 ($p < 0.01$) (Fig. 4b).

To determine whether defective signaling and/or increased apoptosis observed in 2D2 cells can be explained by aberrant surface expression of costimulatory molecules, adhesion molecules, or activation antigens, we examined surface antigens (CD10, CD20, CD29, CD38, CD76, CD80, BAFF-R, and HLA-DR) known to be expressed in Nalm-6 pre-B cells and surface molecules involved in cell adhesion and cell-to-cell interaction (CD9, CD18, CD19, CD24, CD40, CD43, CD47, CD49d, CD49e, CD54, CD62L, and CD81) in wt Nalm-6 cells and $WASP^{-/-}$ 2D2 cells. We observed minimal down-regulation of CD43, HLA-DR, CD19, and CD54 in $WASP^{-/-}$ 2D2 cells (data not shown). These results indicate that impaired cytoskeletal reorganization mediated by CD9 or CD47 and increased apoptosis in 2D2 cells were not due to decrease in CD9, CD47, or in other adhesion molecules.

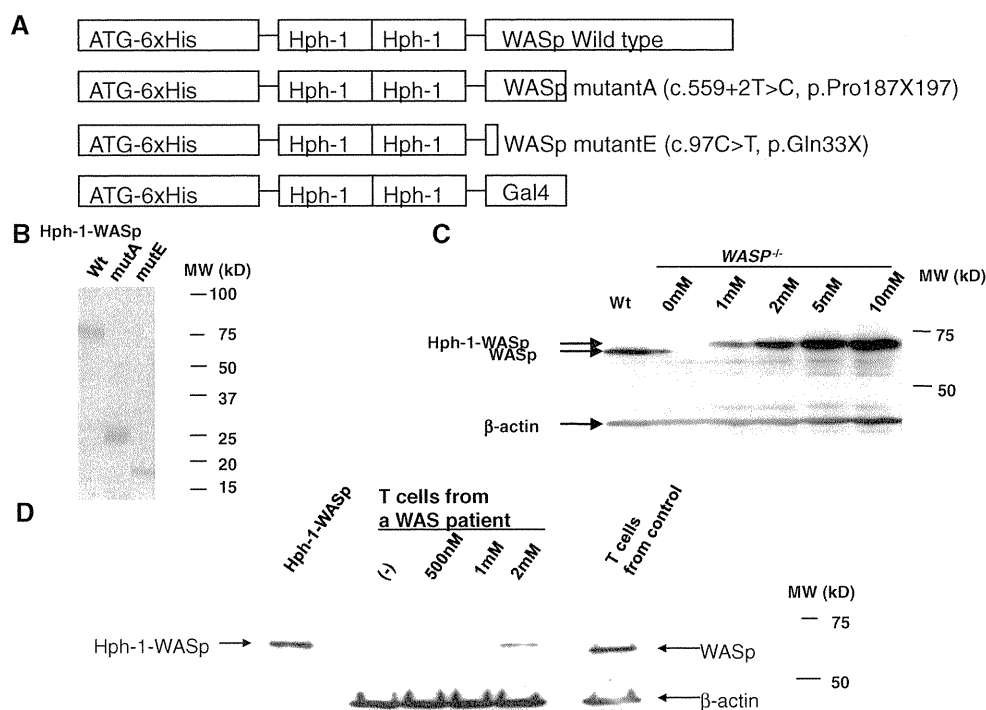## Hph-1-WASp recombinant protein reverses a functional defect of WASp-deficient cells

We then attempted to restore the defective morphological change by forced expression of WASp by protein delivery. Although the protein transduction through a PTD is associated with high efficacy, the recombinant protein fused with PTD sometimes becomes insoluble depending on the nature of the protein. Recombinant WASp is one of such protein species known to become insoluble when expressed in bacteria. We constructed a fusion protein consisting of a PTD of human origin, Hph-1, 6× His for purification, and WASp (wt, mutant A with p. Pro187X197, and mutant E

with pGln33X); Construct shown in Fig. 5a). We included two Hph-1 sequences in tandem to the construct for their enhanced transduction capacity compared to single Hph-1-containing protein. Most of the protein was detected in insoluble fraction in 37°C culture, but close to 5% of the protein was recovered in soluble fraction with expression induction at low temperature overnight in an optimized medium with Rosetta™2 (DE3) pLysS bacteria strain. Coomassie Brilliant Blue (CBB) staining of the protein purified by Ni-resin column showed a major band at 70-kDa that corresponded to Hph-1wtWASp, 25-kDa Hph-1 WASp mutant A, and 18-kDa WASp mutant E (Fig. 5b). The final product was desalted with Microcon filter devices, and used for further experiments.

To determine the kinetics of protein delivery of Hph-1-WASp in $WASP^{-/-}$ cells, the recombinant protein was incubated with 2D2 cells at 10^6 cells/mL at 1, 2, 5, and 10 μM for 1 h in serum-free medium, after which the cells were checked for Hph-1-WASp expression. Figure 5c demonstrates that WASp is transduced in a concentration-dependent fashion. Hph-1-WASp was detectable when transduced at 1 μM, and the expression level was more than that of wt Nalm-6 cells with 2 μM of Hph-1-WASp. Preliminary transduction experiments showed that transduction efficacy of Hph-1 proteins into $WASP^{-/-}$ Nalm-6 cells was more than 95% (data not shown). More importantly, the Hph-1-WASp was expressed in primary T cells from a patient with WAS expanded in vitro with plate-bound anti-CD3 mAb and IL-2 when incubated at 2 μM (Fig. 5d).

We next addressed whether Hph-1-WASp could complement cellular dysfunction of 2D2 cells. 2D2 cells were transduced with either Hph-1-wt WASp, Hph-1-mutant A,

Fig. 5 PTD-WASp prepared in bacteria can be transduced and expressed in WASp-deficient Nalm-6 cells and in T cells from a WAS patient. **a** Schematic structure of Hph-1-wt WASp, -WASp mutants, and -Gal4. **b** Generation of Hph-1-WASp recombinant protein: Hph-1-WASp was produced in bacteria, purified by a Ni-agarose column, eluted by 300 mM imidazole, and desalted. The products were subjected to SDS-PAGE and stained by CBB staining. **c** Hph-1-WASp protein was transduced into WASp$^{-/-}$ Nalm-6 cells in a dose-depende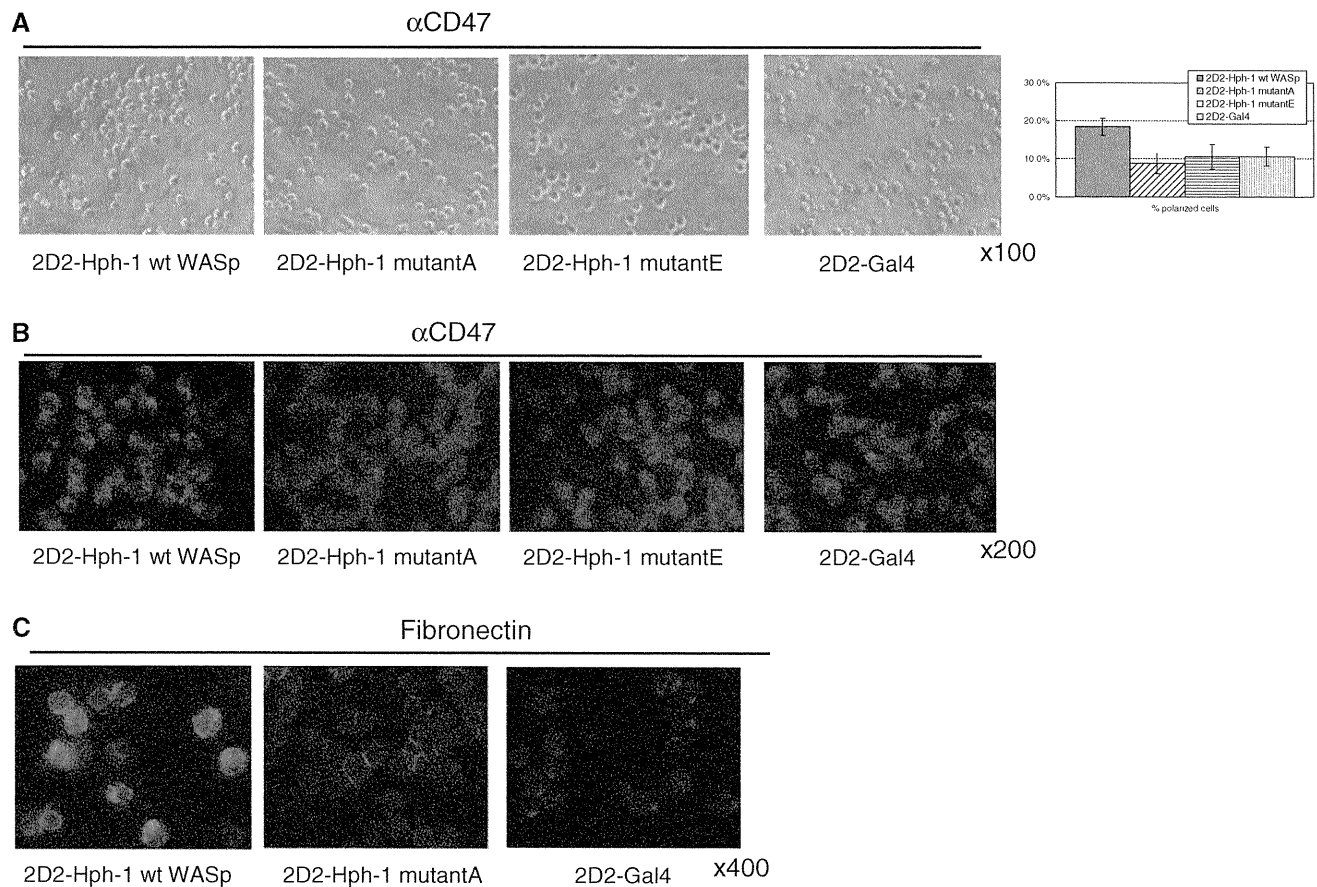nt manner at 1 h after incubation. Hph-1-WASp protein was introduced in 2D2 cells for 1 h at 1, 2, 5, and 10 mM and expression of the exogenous WASp was verified by Western blot analysis. An anti-β-actin blot is shown as a control. **d** Hph-1-WASp was expressed in in vitro expanded primary T cells from a patient with WAS. Hph-1-WASp was incubated at 500 nM, 1 mM, and 2 mM for 1 h with T cells from a patient with WAS expanded in vitro. *Arrows* indicate the position of endogenous WASp of T cells from a normal subject and exogenous WASp transduced by Hph-1. One representative blot out of three independent experiments for different WAS patients is shown

or Hph-1-mutant E at 1 μM for 1 h, washed, and then transferred into anti-CD47 mAb-coated wells. The cells were examined under a microscope at 1 h and the percentage of cells with a spreading morphology was calculated (Fig. 6a). 8.8–10.6% of Hph-1-WASp-negative mutant-transduced 2D2 cells displayed polarization and adhesion to the CD47 mAb-bound plate. The defective morphological changes of WASp-negative Nalm-6 cells were restored by transduction of Hph-1-WASp, 18.4% of transduced 2D2 cells attached to the plate showing actin reorganization, while the cells that expressed Hph-1-Gal4 control protein did not display the improved reorganization (Fig. 6a). Either mutant A or mutant E failed to compensate the defect in the cytoskeletal reorganization. The same observation was made in F-actin staining as shown in Fig. 6b. Similarly, transduction of the recombinant wt WASp but not mutant A or control protein failed to restore actin reorganization elicited by fibronectin (Fig. 6c). These results suggest that the abnormal protein transduction system can be used to delve into the functional aspect of the various WASp mutants and wt WASp.

Discussion

In this study, we generated a *WASP*-disrupted pre-B-cell line and demonstrated defective cell adhesion/polarization and disrupted B-cell signaling upon B-cell surface engagement in the absence of WASp. Alterations in CD47-induced and CD9-induced signaling were demonstrated in *WASP*$^{-/-}$ cells. Our research showed that recombinant WASp in cell-permeable form can be recovered in a soluble fraction with the optimization of culture condition. The transduction of recombinant PTD-WASp was possible in primary cells and restored impaired cell locomotion and cytoskeletal rearrangement in *WASP*$^{-/-}$ Nalm-6 cells.

WASp-deficient pre-B cells exhibited defective cell polarization, a spreading morphology, and altered cell signaling through CD47 receptors, CD9 receptors, and fibronectin stimulation. CD47 is known as an integrin-associated protein which binds to thrombospondin-1 and SHPS-1 [31]. CD47 ligation induces cellular spreading and adhesion, leading to caspase-independent cell death [30]. The receptor ligation, however, does not promote cell death

A   αCD47

2D2-Hph-1 wt WASp   2D2-Hph-1 mutantA   2D2-Hph-1 mutantE   2D2-Gal4   **x100**

B   αCD47

2D2-Hph-1 wt WASp   2D2-Hph-1 mutantA   2D2-Hph-1 mutantE   2D2-Gal4   **x200**

C   Fibronectin

2D2-Hph-1 wt WASp   2D2-Hph-1 mutantA   2D2-Gal4   **x400**

Fig. 6 Transduction of Hph-1-WASp restores the functional deficit in *WASP*-disrupted 2D2 cells. **a** Restoration of adhesion capacity in WASP$^{-/-}$ cells by transduction of Hph-1-WASp and percentage of cells with polarization adhered to wells coated with anti-CD47 mAb: 2D2 cells were incubated in the presence of Hph-1-WASp proteins at 1 mM for 1 h, transferred into anti-CD47-coated wells, and were inspected using inverted microscopy. One representative data out of five independent experiments are shown. Summary of five independent experiments is shown in *right panel*. The experiments were repeated at least twice and the mean and SD was calculated. At least 750 cells were counted in each experiment. *Error bars* indicate SD. **b, c** Defective F-actin accumulation in 2D2 cells was restored by induction of Hph-1-WASp wt protein. 2D2 cells were stained with Rhodamine-phalloidin after induction of Hph-1-WASp proteins following stimulation with anti-CD47 mAb-coated plates for 1 h or with fibronectin for 2 h. F-actin accumulation was observed in 2D2 cells with induction of Hph-1-WASp wt protein, but not in cells with induction of Hph-1-WASp-negative mutant proteins. One representative data out of five (**b**) and three (**c**) independent experiments are shown

in mononuclear cells from patients with WAS [30]. In our study, cell polarization and adhesion triggered by the engagement of the CD47 receptor was affected in WASp-deficient Nalm-6 cells, which mirrors observation made in human mature B-cell lines [30]. On the other hand, mutations in WASP are known to accelerate lymphocytes through upregulation of the Fas-mediated cell death [37]. In concordance with the observation, CD24-mediated apoptosis was augmented in 2D2 pre-B cells. This suggests that the CD24 signal may not contribute to survival of autoreactive B-cell clone in WAS patients. The mechanism of the enhanced CD24-mediated apoptosis warrants further study.

Impaired CD47-mediated signaling was also documented in anti-phosphotyrosine blots of cellular proteins in WASP$^{-/-}$ cells. CD47-driven phosphorylation of Syk was impaired in the absence of WASp. Virtually no change was observed in phosphorylation of Btk, Lyn, and c-Src in WASp-deficient Nalm-6 cells when stimulated with anti-CD47 mAb. Though 4G10 blot showed that tyrosine phosphorylation of cellular substrates is generally enhanced by CD47 engagement in Nalm-6 cells, most of PTKs (Btk, Lyn, and c-Src) except Syk seemed inactivated through CD47 signal in the pre-B-cell line. It may be plausible that the detected phosphorylation was at the negative regulatory tyrosine residue of PTKs. Interactions between SIRPα expressed on phagocytes and CD47 expressed on hematopoietic cells negatively regulate phagocyte activity of macrophages and other phagocytic cells; however, consequences of CD47 signal is not yet clear[38]. An in-depth search for the phosphorylated proteins and phosphorylation sites of the individual PTKs

would help clarify the signal cascade initiated by CD47 engagement in the presence or absence of WASp. In experimental aspects, analysis of signaling abnormalities in the absence of WASp would be feasible with the use of the $WASP^{-/-}$ cell line. PTK activation was induced in wt Nalm-6 cells by CD9 crosslinking, however, the activation was suppressed by the same stimuli in $WASP^{-/-}$ Nalm-6 cells. Although this study did not delve into the signaling pathway through CD9 and CD47 in pre-B cells, the gene-disrupted pre-B-cell line in combination with protein transduction approach would provide us with unique opportunity to study a signal pathway in detail.

In this study, we generated recombinant WASp that can be used for biochemical analysis and protein delivery studies. Previously, the generation of recombinant WASp in prokaryotic expression systems has been attempted in our laboratory [39] as well as in other laboratories [40–42] without much success in large scale generation of full-length WASp. One of the reasons for poor expression, recovery, or both, of recombinant WASp may be related to its binding capacity to cytoskeletal proteins leading to insolubility. Through elaboration of the incubation time, temperature, and choice of host bacteria strain, purification of a sufficient amount of Hph-1-WASp in soluble fraction in a relatively large quantity is now possible. Although it remains to be determined whether the recombinant protein with two-tandem Hph-1s (22 amino acids) correctly folds in the cytoplasmic region and mimics wt WASp in other biochemical studies, the recombinant protein was detected in the cytoplasm (data not shown) and restored the defective actin reorganization in $WASp^{-/-}$ cells. In contrast two mutant WASps failed to compensate for the morphological defects. These indicate that the protein probably retained its native structure. The protein delivery of wt as well as mutant WASp in combination with the WASp-deficient cell line or with WASp-deficient lymphocytes would facilitate in-depth biochemical and functional analysis of WASp mutants. PTD-WASp would be particularly valuable for studies using primary cells, because it was effectively transduced into primary immune cells without affecting viability.

Recent papers report that signals mediated by WASp are essential for regulatory T-cell (Treg) homeostasis, peripheral activation, and in vivo function [43]. WASp-sufficient Tregs manifest a strong in vivo selective advantage, while the defective function of WAS Tregs can be partially rescued by pre-activation with IL-2. Thus, it is yet to be determined whether WASp is important in Treg development or in Treg function. It is of interest to see whether Hph-1-WASp expression in WAS Tregs can restore function and whether it has an effect on inducible Treg development in T cells lacking WASp.

A variety of mutants can be readily generated with our gene-targeting system. This novel system has enabled rapid disruption of virtually any locus of the human genome within 4 weeks and homozygous knockout clones lacking a human gene of interest can be created within 8–12 weeks. Disruption of multiple genes has already been proven feasible. Another feature of this gene-targeting system is its capacity to eliminate drug-resistant cassettes with the Cre-loxP recombination system. With elaborate vector construction and gene-targeting strategies, Nalm-6 cells that harbor the particular mutation without any additional gene modification can be generated. This could serve as a bona fide model cell line which mimics the status of a particular patient.

In this study, we detailed the development of a novel analytical tool that may aid research related to immunodeficiency diseases. Although this study focused on the functional and biochemical aspects of WASp, the combination of human cellular knockouts and PTD would enable the detailed identification and dissection of the biochemical defects associated with genetic disorders, especially those defects responsible for primary immunodeficiency diseases.

References

1. Wiskott A. Familiärer, angeborener Morbus Werlhofii? Monatsschr Kinderheilkd.1937;68:212–16.
2. Aldrich RA, Steinberg AG, Campbell DC. Pedigree demonstrating a sex-linked recessive condition characterized by draining ears, eczematoid dermatitis and bloody diarrhea. Pediatrics. 1954;13:133–9.
3. Derry JM, Ochs HD, Francke U. Isolation of a novel gene mutated in Wiskott–Aldrich syndrome. Cell. 1994;78:635–44.
4. Imai K, et al. Clinical course of patients with WASP gene mutations. Blood. 2004;103:456–64.
5. Jin Y, et al. Mutations of the Wiskott–Aldrich syndrome protein (WASP): hotspots, effect on transcription, and translation and phenotype/genotype correlation. Blood. 2004;104:4010–9.
6. Ochs HD, Thrasher AJ. The Wiskott–Aldrich syndrome. J Allergy Clin immunol. 2006;117:725–38 (quiz 739).
7. Orange JS, Stone KD, Turvey SE, Krzewski K. The Wiskott–Aldrich syndrome. Cell Mol Life Sci. 2004;61:2361–85.
8. Ramesh N, Anton IM, Martinez-Quiles N, Geha RS. Waltzing with WASP. Trends Cell Biol. 1999;9:15–9.

9. Takenawa T, Suetsugu S. The WASP-WAVE protein network: connecting the membrane to the cytoskeleton. Natl Rev Mol Cell Biol. 2007;8:37–48.

10. Anton IM, et al. WIP deficiency reveals a differential role for WIP and the actin cytoskeleton in T and B cell activation. Immunity. 2002;16:193–204.

11. de la Fuente MA, et al. WIP is a chaperone for Wiskott–Aldrich syndrome protein (WASP). Proc Natl Acad Sci USA. 2007;104: 926–31.

12. Baba Y, et al. Involvement of Wiskott–Aldrich syndrome protein in B-cell cytoplasmic tyrosine kinase pathway. Blood. 1999;93: 2003–12.

13. Banin S, Truong O, Katz DR, Waterfield MD, Brickell PM, Gout I. Wiskott–Aldrich syndrome protein (WASp) is a binding partner for c-Src family protein-tyrosine kinases. Curr Biol. 1996;6:981–8.

14. McGavin MK, Badour K, Hardy LA, Kubiseski TJ, Zhang J, Siminovitch KA. The intersectin 2 adaptor links Wiskott Aldrich syndrome protein (WASp)-mediated actin polymerization to T cell antigen receptor endocytosis. J Exp Med. 2001;194:1777–87.

15. Yarar D, D'Alessio JA, Jeng RL, Welch MD. Motility determinants in WASP family proteins. Mol Biol Cell. 2002;13:4045–59.

16. Aspenstrom P, Lindberg U, Hall A. Two GTPases, Cdc42 and Rac, bind directly to a protein implicated in the immunodeficiency disorder Wiskott–Aldrich syndrome. Curr Biol. 1996;6:70–5.

17. Tian L, Nelson DL, Stewart DM. Cdc42-interacting protein 4 mediates binding of the Wiskott-Aldrich syndrome protein to microtubules. J Biol Chem. 2000;275:7854–61.

18. Gerwin N, Friedrich C, Perez-Atayde A, Rosen FS, Gutierrez-Ramos JC. Multiple antigens are altered on T and B lymphocytes from peripheral blood and spleen of patients with Wiskott–Aldrich syndrome. Clin Exp Immunol. 1996;106:208–17.

19. Westerberg L, Larsson M, Hardy SJ, Fernandez C, Thrasher AJ, Severinson E. Wiskott–Aldrich syndrome protein deficiency leads to reduced B-cell adhesion, migration, and homing, and a delayed humoral immune response. Blood. 2005;105:1144–52.

20. Abdul-Manan N, et al. Structure of Cdc42 in complex with the GTPase-binding domain of the 'Wiskott–Aldrich syndrome' protein. Nature. 1999;399:379–83.

21. Facchetti F, et al. Defective actin polymerization in EBV-transformed B-cell lines from patients with the Wiskott–Aldrich syndrome. J Pathol. 1998;185:99–107.

22. Morio T, et al. The increase of non-MHC-restricted cytotoxic cells (gamma/delta-TCR-bearing T cells or NK cells) and the abnormal differentiation of B cells in Wiskott–Aldrich syndrome. Clin Immunol Immunopathol. 1989;52:279–90.

23. Park JY, Kob M, Prodeus AP, Rosen FS, Shcherbina A, Remold-O'Donnell E. Early deficit of lymphocytes in Wiskott–Aldrich syndrome: possible role of WASP in human lymphocyte maturation. Clin Exp Immunol. 2004;136:104–10.

24. Snapper SB, et al. Wiskott–Aldrich syndrome protein-deficient mice reveal a role for WASP in T but not B cell activation. Immunity. 1998;9:81–91.

25. Wada T, Jagadeesh GJ, Nelson DL, Candotti F. Retrovirus-mediated WASP gene transfer corrects Wiskott–Aldrich syndrome T-cell dysfunction. Hum Gene Ther. 2002;13:1039–46.

26. Westerberg L, Greicius G, Snapper SB, Aspenstrom P, Severinson E. Cdc42, Rac1, and the Wiskott–Aldrich syndrome protein are involved in the cytoskeletal regulation of B lymphocytes. Blood. 2001;98:1086–94.

27. Adachi N, et al. The human pre-B cell line Nalm-6 is highly proficient in gene targeting by homologous recombination. DNA Cell Biol. 2006;25:19–24.

28. Iiizumi S, et al. Simple one-week method to construct gene-targeting vectors: application to production of human knockout cell lines. Biotechniques. 2006;41:311–6.

29. Choi JM, et al. Intranasal delivery of the cytoplasmic domain of CTLA-4 using a novel protein transduction domain prevents allergic inflammation. Nat Med. 2006;12:574–9.

30. Mateo V, et al. Mechanisms of CD47-induced caspase-independent cell death in normal and leukemic cells: link between phosphatidylserine exposure and cytoskeleton organization. Blood. 2002;100:2882–90.

31. Motegi S, et al. Role of the CD47-SHPS-1 system in regulation of cell migration. EMBO J. 2003;22:2634–44.

32. Ellerman DA, et al. Direct binding of the ligand PSG17 to CD9 requires a CD9 site essential for sperm–egg fusion. Mol Biol Cell. 2003;14:5098–103.

33. Schurman SH, Candotti F. Autoimmunity in Wiskott–Aldrich syndrome. Curr Opin Rheumatol. 2003;15:446–53.

34. Suzuki T, Kiyokawa N, Taguchi T, Sekino T, Katagiri YU, Fujimoto J. CD24 induces apoptosis in human B cells via the glycolipid-enriched membrane domains/rafts-mediated signaling system. J Immunol. 2001;166:5567–77.

35. Taguchi T, et al. Pre-B cell antigen receptor-mediated signal inhibits CD24-induced apoptosis in human pre-B cells. J Immunol. 2003;170:252–60.

36. Taguchi T, et al. Deficiency of BLNK hampers PLC-gamma2 phosphorylation and Ca2+ influx induced by the pre-B-cell receptor in human pre-B cells. Immunology. 2004;112:575–82.

37. Rengan R, et al. Actin cytoskeletal function is spared, but apoptosis is increased, in WAS patient hematopoietic cells. Blood. 2000;95:1283–92.

38. Matozaki T, et al. Functions and molecular mechanisms of the CD47-SIRPα signaling pathway. Trends Cell Biol. 2009;19: 72–80.

39. Imai K, et al. The pleckstrin homology domain of the Wiskott–Aldrich syndrome protein is involved in the organization of actin cytoskeleton. Clin Immunol. 1999;92:128–37.

40. Cory GO, Garg R, Cramer R, Ridley AJ. Phosphorylation of tyrosine 291 enhances the ability of WASp to stimulate actin polymerization and filopodium formation. Wiskott–Aldrich syndrome protein. J Biol Chem. 2002;277:45115–21.

41. Myers SA, Leeper LR, Chung CY. WASP-interacting protein is important for actin filament elongation and prompt pseudopod formation in response to a dynamic chemoattractant gradient. Mol Biol Cell. 2006;17:4564–75.

42. Westerberg LS, et al. Activating WASP mutations associated with X-linked neutropenia result in enhanced actin polymerization, altered cytoskeletal responses, and genomic instability in lymphocytes. J Exp Med. 2010;207:1145–52.

43. Humblet-Baron S, et al. Wiskott–Aldrich syndrome protein is required for regulatory T cell homeostasis. J Clin Invest. 2007; 117:407–18.

44. Morio T, et al. Ku in the cytoplasm associates with CD40 in human B cells and translocates into the nucleus following incubation with IL-4 and anti-CD40 mAb. Immunity. 1999;11: 339–48.

45. Morio T, Nagasawa M, Nonoyama S, Okawa H, Yata J. Phenotypic profile and functions of T cell receptor-gamma delta-bearing cells from patients with primary immunodeficiency syndrome. J Immunol. 1990;144:1270–5.
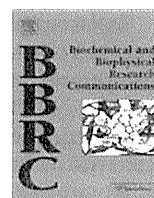
Transducible form of p47^{phox} and p67^{phox} compensate for defective NADPH oxidase activity in neutrophils of patients with chronic granulomatous disease

Fumiko Honda [a], Yumiko Hane [a], Tomoko Toma [b], Akihiro Yachie [b], Eun-Sung Kim [c], Sang-Kyou Lee [c], Masatoshi Takagi [a], Shuki Mizutani [a], Tomohiro Morio [a,*]

[a] Department of Pediatrics and Developmental Biology, Tokyo Medical and Dental University Graduate School of Medical and Dental Sciences, Tokyo, Japan
[b] Department of Pediatrics, Kanazawa University School of Medicine, Kanazawa, Japan
[c] Department of Biotechnology, Yonsei University, Seoul, Republic of Korea

ARTICLE INFO

ABSTRACT

Protein delivery to primary cells by protein transduction domain (PTD) serves as a novel measure for manipulation of the cells for biological study and for the treatment of various human conditions. Although the method has been employed to modulate cellular function *in vitro*, only limited reports are available on its application in the replacement of deficient signaling molecules into primary cells. We examined the potential of recombinant proteins to compensate for defective cytosolic components of the NADPH oxidase complex in chronic granulomatous disease (CGD) neutrophils in both p47^{phox} and p67^{phox} deficiency. The p47^{phox} or p67^{phox} protein linked to Hph-1 PTD was effectively expressed in soluble form and transduced into human neutrophils efficiently without eliciting unwanted signal transduction or apoptosis. The delivered protein was stable for more than 24 h, expressed in the cytoplasm, translocated to the membrane fraction upon activation, and, most importantly able to restored reactive oxygen species (ROS) production. Although research on human primary neutrophils using the protein delivery system is still limited, our data show that the protein transduction approach for neutrophils may be applicable to the control of local infections in CGD patients by direct delivery of the protein product.

© 2011 Elsevier Inc. All rights reserved.

1. Introduction

Chronic granulomatous disease (CGD) is a primary immunodeficiency that affects phagocytes of the innate immune system and is characterized by recurrent life-threatening bacterial and fungal infections. The disease is caused by the lack of a component of NADPH oxidase complex [1]. NADPH oxidase is a multicomponent enzyme that is critical in non-mitochondrial ROS production, and is composed of a flavocytochrome b558 (gp91^{phox} and p22^{phox}), cytosolic components (p40^{phox}, p47^{phox}, and p67^{phox}) and a small GTP-binding protein (Rac1 or Rac2) [2]. About 60% of CGD cases are caused by mutations in the gene encoding gp91^{phox} located on X chromosome. Mutation in *NCF1* (encoding p47^{phox}) causes the most common autosomal recessive form of CGD accounting for approximately 20% of all CGD cases. Mutation in *NCF2* (encoding p67^{phox}) accounts for about 5% of all CGD cases [1,3]. Hematopoietic cell transplantation is currently the only proven curative therapy, but is often associated with transplant-related mortality [1,4]. There

has been no effective therapeutic method to modulate neutrophil function or to reconstitute the functional defects in CGD neutrophils.

The intracellular delivery of proteins or peptides, has been difficult to achieve until recently, primarily due to plasma membrane barrier restrictions on the uptake of macromolecules. Cell penetrating peptide or protein transduction domain (PTD) is a short peptide of generally fewer than 30 amino acids that can cross biological membranes in a receptor- and cell-cycle-independent manner [5–7]. PTD is especially useful for delivery of large molecules into transfection-resistant cells, and can be incorporated into virtually any types of cells [5,8,9].

The protein transduction technique has most commonly been employed for modulation of specific protein–protein interactions with target transcription factors, signal transduction proteins, and cell cycle mediators [10]. Specific proteins and peptides for therapeutic targeting of oncogenes have been developed and tested *in vitro* and with *in vivo* animal models [10,11]. The protein transduction approach has also been used for delivery of active enzymes or other functional molecules in neurodegenerative disorders and metabolic diseases. PTD enzyme replacement *in vitro* has been successfully demonstrated in many previous publications [12–14]; however, their potential advantage as a method for intracellular replacement therapy *in vivo* is still largely unknown.

* Corresponding author. Address: Department of Pediatrics and Developmental Biology, Tokyo Medical and Dental University Graduate School of Medical and Dental Sciences, 1-5-45 Yushima, Bunkyo-Ku, Tokyo 113-8519, Japan. Fax: +81 3 5803 5245.
E-mail address: tmorio.ped@tmd.ac.jp (T. Morio).

Replacement of functional signaling molecules by PTD techniques in cells is more technically demanding than delivery of protein–protein interaction modulators or active enzymes. This is because, in PTD, the delivered protein should be expressed at a physiological level, targeted to the specific cellular location, associated with other molecules, modified and translocated upon stimulation, and biologically active as long as the endogenous molecule.

The objective of this study was to compensate neutrophil dysfunction in CGD lacking a cytosolic component of the NADPH oxidase complex by the protein delivery system using Hph-1, an 11-amino acid long unique peptide of human origin, as PTD [15,16]. To achieve this, the transduced protein should function as its endogenous counterpart inside the cells. Activation of the complex is tightly controlled by plasma membrane targeting and/or phosphorylation of the cytosolic components [2,17]. Upon priming signal that activates PI3K, Rac2 released from GDP-dissociation inhibitor translocates to the membrane. During activation, p47 is phosphorylated on multiple Serines by PKC, leading to the translocation of the p47/p67/(p40) complex to the membrane [2,17,18]. The cytosolic components should locate in the cytoplasm in resting state, receive modification upon activation, associate with other molecules, and translocate to the membrane.

We also investigated possibility of the protein transduction to activate, or induce apoptosis in, neutrophils. Neutrophils have a short lifespan in the periphery and ex vivo, and the cells are quickly responsive and sensitive to the external stimuli, all factors that render cell manipulation even more difficult. Neutrophils sense microbes through various receptors, engulf foreign bodies, and are destined to undergo apoptosis after production of reactive oxygen species (ROS) and releasing neutrophil extracellular traps [19,20]. It has been postulated that PTD-mediated delivery of macromolecules does not elicit the innate immune response or cytotoxicity [9,10,13], but, to our knowledge, the cellular reactions elicited by protein delivery has not been formally addressed in human neutrophils.

We show here evidence that PTD-based protein delivery does not elicit non-specific activation or apoptosis of human neutrophils. We show that transduced recombinant p47 or p67 protein linked to Hph-1 distributes to a physiological location (i.e., moving to the plasma membrane) and restores normal ROS production in CGD neutrophils deficient in p47 or p67, respectively.

2. Results

2.1. Transduction efficacy of recombinant protein into human neutrophils and its effect on neutrophil activation and apoptosis
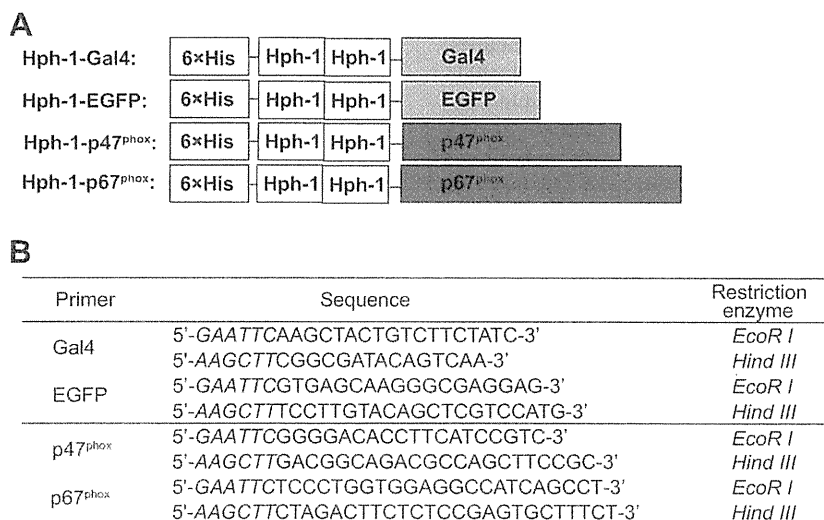
We first generated a construct for Hph-1-EGFP as a control protein for assessing expression kinetics, activation, and cellular apoptosis in neutrophils following protein transduction (Fig. 2A). The EGFP recombinant was expressed in bacteria, purified, treated with polymyxin B, and incubated with 1×10^6 purified human neutrophils with various concentrations and for various time periods. The recombinant was similarly incubated with human activated T-cells (CD3+ ≥95%) and with human B-cell line (i.e., Daudi cells).

The kinetics study monitored by flow cytometer showed the expression level at 10 min was higher in neutrophils compared to that in activated T-cells and Daudi cells. In neutrophils, the expression level reached a maximum by 30 min; and ≥95% of the recombinant protein was expressed, while in activated T-cells the level peaked at 60 min (Fig. 3A).

The transduced protein was easily detectable in the cytoplasm at 1 μM by confocal fluorescence microscopy (CFM) as well as by flow cytometer, and the expression was increased in a dose dependent fashion (Fig. 3B and C). The dose–response was similar to that in Daudi cells; but significantly more EGFP protein was detected in neutrophils than in activated T-cells. The expression was detected at least up until 24 h post-Hph-1-EGFP transduction, suggesting that no major biodegradation of incorporated protein occurred (Fig. 3D).
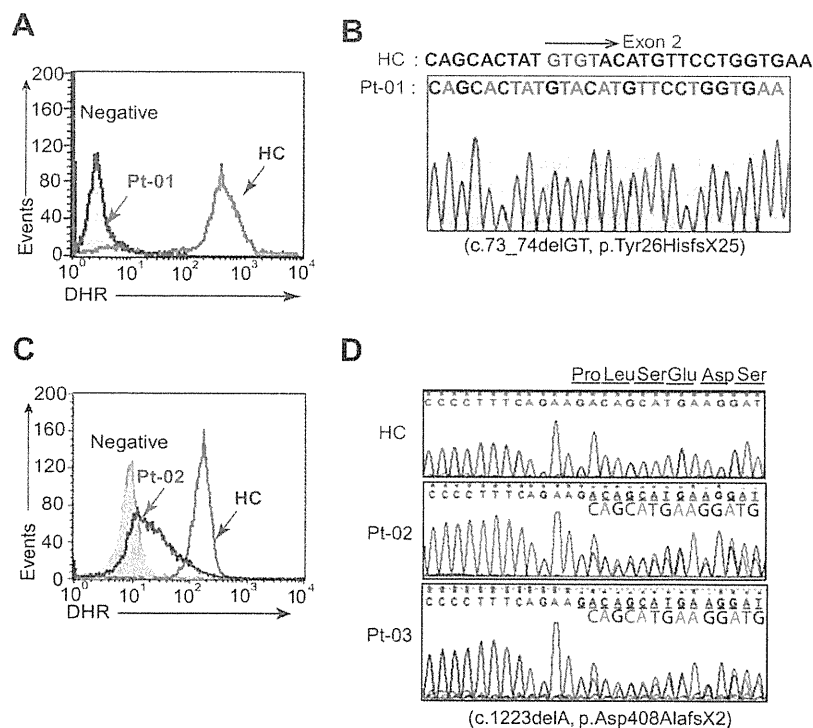
Fig. 1. Diagnosis of CGD in patients 1, 2, and 3 by assessment of ROS production and by sequencing analysis. (A and C) A representative FACS histogram for assessment of ROS production, measured by DHR123 fluorescence in purified neutrophils from healthy control (HC), p47-deficiency patient (Pt-01) (A) and from p67 deficiency (Pt-02) (C). (B and D) A result of sequencing analysis of NCF1 in Pt-01 (B) and NCF2 in Pt-02 and Pt-03 (D).

A

Hph-1-Gal4:	6×His	Hph-1	Hph-1	Gal4
Hph-1-EGFP:	6×His	Hph-1	Hph-1	EGFP
Hph-1-p47^{phox}:	6×His	Hph-1	Hph-1	p47^{phox}
Hph-1-p67^{phox}:	6×His	Hph-1	Hph-1	p67^{phox}

B

Primer	Sequence	Restriction enzyme
Gal4	5'-GAATTCAAGCTACTGTCTTCTATC-3'	EcoR I
	5'-AAGCTTCGGCGATACAGTCAA-3'	Hind III
EGFP	5'-GAATTCGTGAGCAAGGGCGAGGAG-3'	EcoR I
	5'-AAGCTTTCCTTGTACAGCTCGTCCATG-3'	Hind III
p47^{phox}	5'-GAATTCGGGGACACCTTCATCCGTC-3'	EcoR I
	5'-AAGCTTGACGGCAGACGCCAGCTTCCGC-3'	Hind III
p67^{phox}	5'-GAATTCTCCCTGGTGGAGGCCATCAGCCT-3'	EcoR I
	5'-AAGCTTCTAGACTTCTCTCCGAGTGCTTTCT-3'	Hind III

Fig. 2. Schematic diagram of Hph-1-recombinant constructs. (A) Schematic diagram of Hph-1-Gal4, Hph-1-EGFP, Hph-1-p47^{phox}, and Hph-1-p67^{phox}. (B) Primer sequences for construction of the indicated Hph-1-recombinant protein.

We next examined whether the transduction of foreign protein *per se* activates neutrophils or potentially elicits cellular damage leading to augmented or earlier apoptosis. Fig. 3D shows that the proportion of apoptotic cells does not increase in neutrophils transduced with Hph-1-EGFP compared to untreated neutrophils. Induction of Hph-1-EGFP did not induce significant activation of tyrosine kinases, activation of Akt, or phosphorylation of the intracellular components of the NADPH oxidase complex (Fig. 3E). Similarly, ROS production was not observed upon transduction with Hph-1-EGFP protein in addition to fMLP in control neutrophils.

The similar results were obtained when neutrophils were treated with Hph-1-Gal4 (data not shown).

2.2. Hph-1-p47^{phox} and Hph-1-p67^{phox} compensate for defective NADPH oxidase activity in neutrophils of autosomal recessive CGD patients

We hypothesized that restoring intracellular p47 or p67 by protein delivery would correct defective NADPH activity, if the transduced protein were functional. To test this, we designed constructs
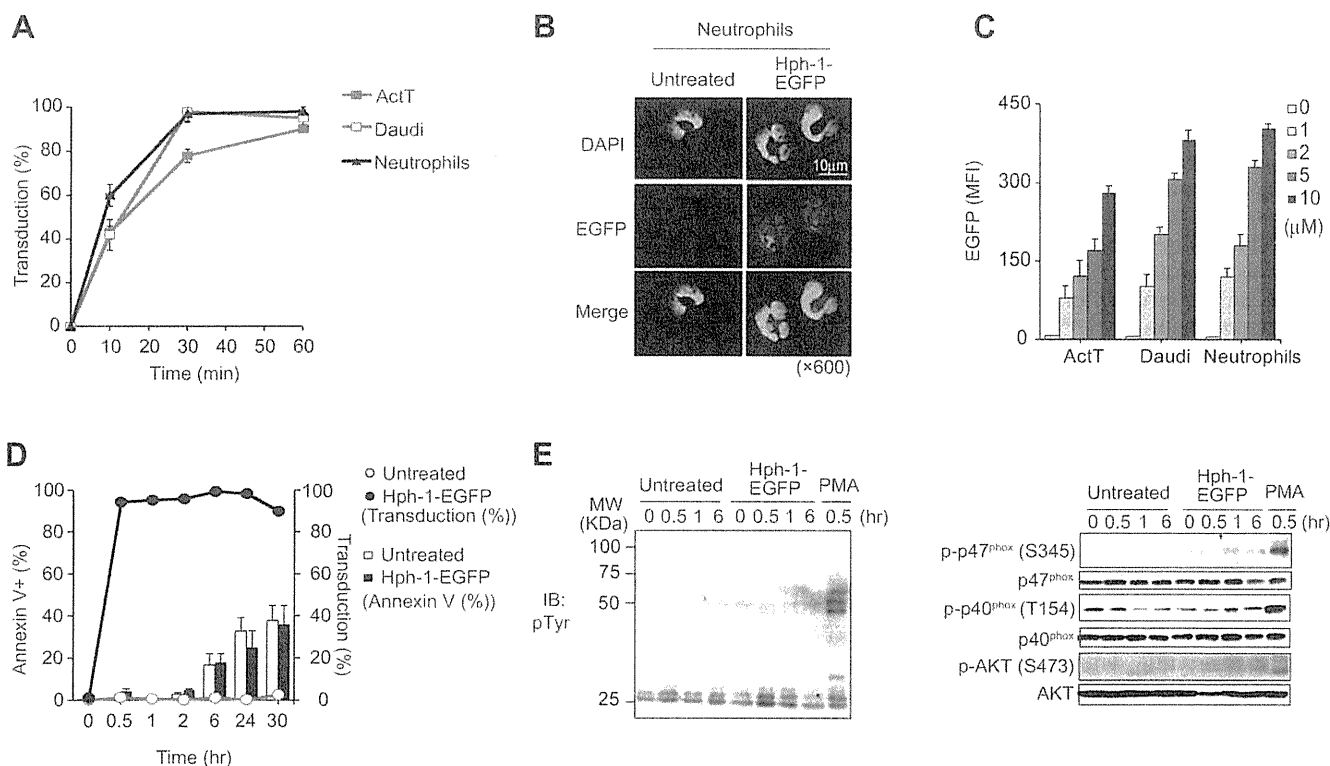
Fig. 3. Time-dependent and concentration-dependent transduction of Hph-1-EGFP in human neutrophils, and the effect of transduction on cellular activation and apoptosis. (A) Time dependent transduction kinetics of Hph-1-EGFP in human neutrophils, activated T-cells (ActT), and Daudi cells. (B) CFM analysis of transduced protein. (C) Concentration dependent intracellular delivery of EGFP in human neutrophils, activated T-cells (ActT), and Daudi cells (n = 3). (D) Percentage of neutrophil apoptosis and EGFP-positivity after EGFP protein delivery. Summary of three independent experiments is shown. (E) Tyrosine phosphorylation of neutrophil proteins, activation of AKT, or phosphorylation of cytosolic factors of NADPH oxidase complex after transduction of Hph-1-EGFP. One representative Western blot out of three independent experiments is shown. Mean + SD is indicated in (A, C, and D).

for Hph-1-p47^{phox} and Hph-1-p67^{phox} (Fig. 2A) and investigated their capacity to confer the ability to produce ROS in CGD neutrophils either lacking in p47 or p67. Hph-1-p47^{phox} and Hph-1-p67^{phox} were expressed abundantly and recovered insoluble fraction in BL21DE3 Escherichia coli strain at 37 °C incubation (Fig. 4A).

To determine the efficacy of transduction, the p47 protein was incubated with 10^6 purified neutrophils from p47-deficiency at various concentrations, and their expression was checked by Western blotting (Fig. 4B). The expression level of p47 was equivalent to that in control neutrophils when incubated at 1–5 μM for 30 min.

To confirm that Hph-1 induced p47 into the cells, we carried out CFM and Western blotting. CFM visualized the presence of p47 in the cytoplasm prior to stimulation, and the colocalization of p47 and gp91 at the membrane after PMA treatment in >95% of the cells (Fig. 4C). We also prepared cytoplasmic and membrane fractions from Hph-1-p47^{phox} transduced neutrophils and carried out anti-p47 Western blotting. The analysis further confirmed that the incorporated p47 protein, and endogenous p67, were located in the cytoplasm, but not in the membrane (Fig. 4C).

We then asked whether the transduced Hph-1-p47^{phox} was functional by measuring PMA-induced ROS production in the neutrophils from Pt-01. The Hph-1-p47^{phox} delivery restored the capacity to generate ROS in p47-deficient CGD neutrophils, while the additional expression did not result in augmented ROS release in control neutrophils (Fig. 4D). Transduction of the p47 recombinant did not enhance apoptosis as examined by Annexin V staining until 24 h post protein delivery (Fig. 4E). The delivery did not induce cellular activation in neutrophils detected by anti-phosphotyrosine blot (Fig. 4F). In addition, the transduced p47 was still detectable at 24 h as observed in Hph-1-EGFP transduction.

Five-times more expression of p67 was observed in p67-deficient neutrophils compared to control neutrophils when Hph-1-p67^{phox} was incubated at 5 μM for 30 min (Fig. 4G). The p67 expression was observed in >90% of the transduced cells by enumeration under CFM. DHR123 assay and luminol assay demonstrated that the intracellular delivery of p67 protein via Hph-1 restored the capacity to generate ROS in response to PMA in p67-deficient CGD neutrophils (Fig. 4H and I). ROS production in the transduced cells was slightly reduced compared to normal neutrophils, when the expression level of the recombinant was adjusted to the level of endogenous p67 (by incubation at 1 μM), but the difference was not statistically significant (Fig. 4H and I). Neither apoptosis nor ROS production was observed in control neutrophils transduced with Hph-1-p67^{phox}.

3. Discussion

In this paper, we have demonstrated that Hph-1-based protein delivery restores neutrophil ROS production in p47^{phox}-deficient and p67^{phox}-deficient CGD patients. The Hph-1-p47^{phox} and Hph-1-p67^{phox} was recovered in soluble fraction in large quantity in bacteria, and the transduction efficacy to neutrophils was at least more than 80%. The transported protein was localized in the cytosol of neutrophils and was translocated, upon stimulation, to the membrane associating with flavocytochrome b558 to cause the activation of NADPH oxidase. The cellular concentration of the recombinant was observed in a concentration-dependent manner, and thus was adjustable to the target level of choice. The PTD-mediated protein delivery per se did not trigger neutrophil activation or affect neutrophil cell survival.

To date, many groups in wide arenas of clinical and basic biology are working toward PTD-based delivery of therapeutic molecules. The diseases being treated in vitro or in vivo animal systems range from cancer, ischemia, neurodegenerative disease, and enzyme deficiency [8,11,14]. Despite the notable successes and high expectations, the use of PTD to deliver proteins has yet to become common place in cell biology, especially in fields using primary cells. This can be ascribed to inefficient protein expression, insolubility of protein, and biodegradation in transduced cells. In particular, research on primary neutrophils using protein delivery system has been limited; and most of the existing research employed peptide fragments for functional modulation of neutrophils [21,22].

Correction of defective molecule in neutrophils has not yet been attempted with PTD-based approach, much less for the replacement of cytoplasmic protein defective in CGD phagocytes. A pioneering work by Polack et al. has shown that the Pseudomonas aeruginosa strain harboring a plasmid encoding ExoS-N-terminal p67 fusion protein, CHA-pBP31, can infect an EBV-transformed cell line from p67-deficient CGD [23]. CHA-pBP31 was able to reconstitute the NADPH oxidase activity, to approximately 40% of normal at MOIs of 5 or 10. The system, however, is labor-intensive, has limits in deliverable molecular size, and is toxic at higher MOI. However, the intracellular delivery of p67 protein can now be achieved more easily, safely, effectively, and in more controlled manner with our PTD-based system.

The only curative therapies available for CGD are hematopoietic cell transplantation and gene therapy, both of which are associated with therapy-related toxicity and adverse effects [1,4]. In addition, infection control is critically important for the success of these curative therapies [1,4]. The true potential of the Hph-1-p47^{phox} and Hph-1-p67^{phox} as a therapeutic measure to correct deficient ROS production is yet to be tested in animal models. This protein delivery can be used, however, in local control of infection of the CGD patients, for example, by using as an ointment, or by applying the protein directly to the site of infection.

PTD-based enzyme replacement therapy has been proven effective in only limited cases or primary immunodeficiency. Purine nucleotide phosphorylase (PNP) is an intracellular enzyme critical for purine degradation, and PNP defects result in severe T-cell immunodeficiency. One study has reported that PNP fused to TAT rapidly enters PNP-deficient lymphocytes and increases intracellular enzyme activity for 96 h [12]. The same group has demonstrated in PNP$^{-/-}$ mice that TAT induced rapid and efficient delivery of active PNP into many tissues, including the brain, leading to correction of metabolic diseases and immune defects [13].

The protein transduction system thus can be applied for the correction of other immuno deficiencies lacking the intracellular enzyme or cytoplasmic signal molecule, either in part or entirely. The examples include severe congenital neutropenia due to mutation in HAX1, ELA2, or MPO and severe combined immunodeficiency caused by mutation in JAK3, LCK, DCLRE1C, NHEJ1, and LIGIV. Although the efficacy and safety should be examined in detail with an in vivo animal model system, clinical applications of these approaches would become a useful therapeutic option, until the time the patients receive curative therapy (e.g., hematopoietic cell transplantation or gene therapy). The unique ability of PTD will facilitate the design of therapeutic proteins that are defective in primary immunodeficiency.

4. Materials and methods

4.1. Case presentation

Pt-01 is 31-year-old female with recurrent skin infection, otitis, and genital candidiasis. She developed CGD colitis at the age of 19. PMA-driven ROS production of neutrophils as assessed by DHR123 staining is minimal (Fig. 1A). Sequencing analysis of the four NADPH oxidase genes (CYBA, CYBB, NCF1, and NCF2) revealed the homozygous c.73_74delGT mutation in NCF1 (Fig. 1B).
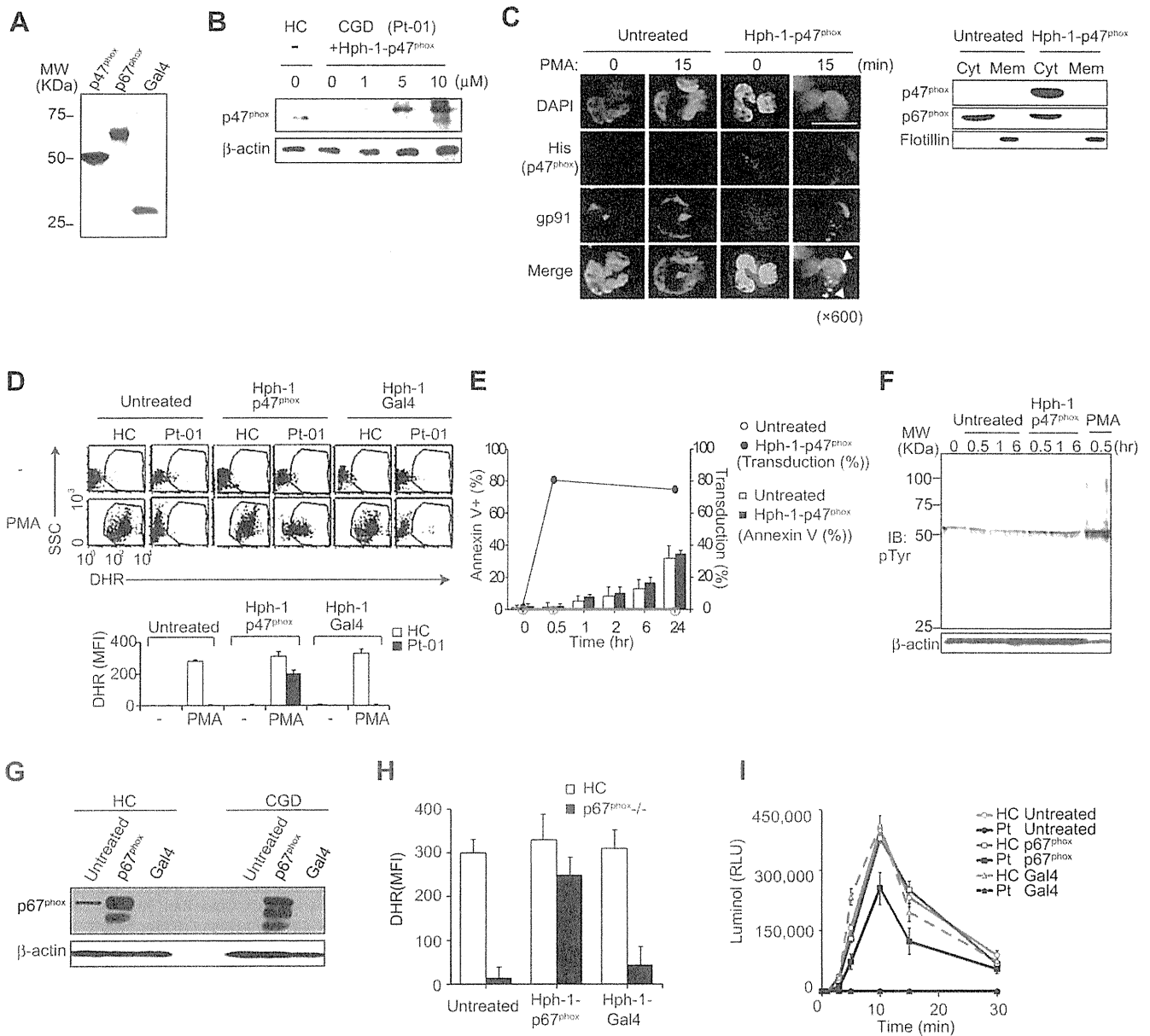
Fig. 4. The delivery of a cytosolic factor of NADPH oxidase complex via Hph-1 PTD results in the expression in the cytoplasm, co-localization with gp91 in the membrane upon stimulation, and restored ROS production in neutrophils from p47- and p67-deficiency. (A) Coomassie Brilliant Blue staining of the purified Hph-1-p47^{phox}, -p67^{phox}, and -Gal4 protein. (B) Expression of p47 in control neutrophils and in p47 deficiency transduced with indicated concentration of Hph-1-p47^{phox}. A representative data out of three independent experiments is shown. Actin is shown as a loading control. (C). Intracellular localization of transduced p47 assessed by CFM (left panel) and by WB (right panel). Flotillin was used as a membrane marker. (D) ROS production assessed by DHR123 staining in control neutrophils and in p47-deficient neutrophils that were transduced with Hph-1-p47^{phox} or with Hph-1-Gal4, and were stimulated as indicated. DMSO was used as a control reagent. Summary of three independent experiments is shown in the lower panel. (E) Percentage of apoptotic cells and p47-expressing cells in p47-negative CGD neutrophils incubated with or without Hph-1-p47^{phox}. Apoptosis was assessed by Annexin V staining, and percentage of p47-positive cells was enumerated by counting the cells with cytoplasmic p47 expression under CFM. (F) Anti-phosphotyrosine blot following transduction of Hph-1-p47^{phox} in p47-deficient neutrophils. (G) Expression of p67 in neutrophils from HC and from p67-deficiency with or without transduction of indicated recombinant protein. One representative data out of three independent experiments for Pt-02 and Pt-03 is shown. (H) Mean DHR123 fluorescence in control neutrophils and in p67-deficient neutrophils, transduced with or without the indicated recombinant. Combined results from three independent experiments for Pt-02 and Pt-03 are shown. (I) Time course of PMA-driven H_2O_2 production, measured by a luminol assay, in control neutrophils and p67-deficiency neutrophils with or without Hph-1-p67^{phox} transduction. One representative data is shown. The experiment was repeated three times in three HCs and p67 deficient patient (Pt-02). HC: healthy control. Mean + SD is shown in D, E, H, and I.

Pt-02 is 8-year-old boy who developed perianal abscess and cervical lymphoadenopathy at 1-year old. Bacterial culture of the abscess revealed the presence of *Serratia marcescens* and Group A *Streptococci*. The DHR123 assay revealed positive but significantly attenuated ROS production (Fig. 1C). Sequencing of the four NADPH oxidase genes revealed a homozygous c1233delA mutation in *NCF2* (Fig. 1D).

Pt-03 is currently 2-year-old girl and is a younger sister of Pt-02. The patient harbored the same mutation in *NCF2* detected in

Pt-02. Pt-03 was well until 2-months old when she developed diarrhea of unknown origin lasting for >8 weeks. Pt-02 and Pt-03 have been on Sulfamethoxazole-Trimethoprim and Itraconazole after diagnosis of CGD and have been well without major infection. However, perianal abscess frequently recurs in Pt-02.

Written informed consent was obtained from all subjects (or their parents). The study protocol was approved by the ethics committee of the Faculty of Medicine, Tokyo Medical and Dental University.

4.2. Reagents

Anti-phosphotyrosine mAb (4G10) and rabbit polyclonal antibody to gp91^{phox} were from Upstate. Mouse mAb to flotillin-1, p67^{phox}, and isotype-matched FITC-mouse IgG were from BD Pharmingen. Mouse mAbs to phospho-AKT, to p47^{phox} were from Rockland Immunochemicals, and from Santa-Cruz, respectively. MAbs to 6x His and to phospho-p40^{phox} were obtained from Cell signaling technology. Antibody directed against phosphor-Ser345 was generated in rabbits by injection with ovalbumin conjugated to the phosphopeptide sequence of p47^{phox} (QARPGPQS [phospho]PGSPLEEE). PMA, dihydrorhodamine 123 (DHR123), DAPI, and luminol were from Sigma–Aldrich.

4.3. Sequencing of NCF1 and NCF2

Sequencing was performed for all exons and exon–intron boundaries of NCF1 and NCF2 as previously described [24] using ABI310 automated genetic analyzer using NCF1 and NCF2 specific primers.

4.4. Isolation of peripheral blood neutrophils

Neutrophils were purified using a standard technique from heparinized peripheral blood using MonoPoly mixture (Flow Laboratories, McLean, VA). The neutrophil-enriched fraction was further purified to >97% by immunomagnetic negative selection (StemCell Technologies). All procedures were carried out under sterile and endotoxin-free conditions.

Subcellular fractionation of neutrophils was carried out according to standard technique previously described. Flotillin was used as a membrane marker.

4.5. Preparation of activated T-cells

Activated T-cells were prepared by incubating peripheral blood mononuclear cells in an OKT3-coated flask in the presence of 350 U/ml IL-2 as previously described [24].

4.6. Measurement of ROS production

Purified neutrophils were loaded with DHR123 at 5 μg/mL for 5 min at 37 °C. Cells were washed, stimulated with PMA (100 ng/ml for 30 min at 37 °C), and ROS production was quantified via flow cytometry (FACSCalibur, Becton Dickinson) by measuring intracellular rhodamine. Alternatively, ROS production was quantified using a standard chemiluminescence method.

4.7. Generation and purification of Hph-1-fusion protein and protein transduction

Hph-1-protein constructs were generated by using the primers shown in Fig. 2B. EGFP, p47^{phox}, and p67^{phox} were amplified from pEGFP-N1 plasmid, NCF-1 cDNA clone (FCC117E05 obtained from TOYOBO), and cDNA from control peripheral lymphocytes, respectively. The amplified fragment and Hph-1 was combined and cloned into pET28b (+) plasmid (Novagen) as previously described. Gal4 construct was described elsewhere.

Protein induction was carried out as previously described [16]. Prepared protein was treated with Detoxi-Gel™ Endotoxin Removing gel (Takara Bio) to eliminate endotoxin.

The cells were incubated with Hph-1 recombinants in PBS at indicated concentrations for indicated time, washed and then were subjected to further analysis.

4.8. Western blotting

Neutrophil lysates were prepared using a lysis buffer (50 mM Tris–HCl, pH 7.5, 150 mM NaCl, 0.25 M sucrose, 5 mM EGTA, 5 mM EDTA, 15 μg/ml leupeptin, 10 μg/ml pepstatin, 10 μg/ml aporotinin, 2.5 mM PMSF, 1.0% NP-40, 0.25% sodium deoxycholate, 10 mM sodium pyrophosphate, 25 mM NaF, 5 mM Na$_3$VO$_4$, 25 mM β-glycerophosphate). Western blotting was carried out as described previously [25].

4.9. Immunofluorescence staining

Cytospin preparations of neutrophils were air-dried and fixed for 10 min with paraformaldehyde in PBS, and then permeabilized using acetone at −20 °C for 20 min, washed, and incubated with the indicated antibodies. Nuclei were counterstained with DAPI. The slides were analyzed with a fluorescence microscope (FV10i, Olympus) equipped with Fluoview viewer and review station.

4.10. Statistical analysis

Student's t-test was used for statistical analysis.

Acknowledgments

References

[1] R.A. Seger, Modern management of chronic granulomatous disease, Br. J. Haematol. 140 (2008) 255–266.
[2] G.M. Bokoch, B. Diebold, J.S. Kim, D. Gianni, Emerging evidence for the importance of phosphorylation in the regulation of NADPH oxidases, Antioxid. Redox Signal. 11 (2009) 2429–2441.
[3] J.A. Winkelstein, M.C. Marino, R.B. Johnston Jr., J. Boyle, J. Curnutte, J.I. Gallin, H.L. Malech, S.M. Holland, H. Ochs, P. Quie, R.H. Buckley, C.B. Foster, S.J. Chanock, H. Dickler, Chronic granulomatous disease. Report on a national registry of 368 patients, Medicine (Baltimore) 79 (2000) 155–169.
[4] B.H. Segal, P. Veys, H. Malech, M.J. Cowan, Chronic granulomatous disease: lessons from a rare disorder, Biol. Blood Marrow Transplant. 17 (2011) S123–S131.
[5] S.R. Schwarze, K.A. Hruska, S.F. Dowdy, Protein transduction: unrestricted delivery into all cells?, Trends Cell Biol. 10 (2000) 290–295.
[6] J.S. Wadia, S.F. Dowdy, Protein transduction technology, Curr. Opin. Biotechnol. 13 (2002) 52–56.
[7] J.M. Gump, S.F. Dowdy, TAT transduction: the molecular mechanism and therapeutic prospects, Trends Mol. Med. 13 (2007) 443–448.
[8] G.P. Dietz, M. Bahr, Delivery of bioactive molecules into the cell: the Trojan horse approach, Mol. Cell. Neurosci. 27 (2004) 85–131.
[9] T. Yoshikawa, T. Sugita, Y. Mukai, Y. Abe, S. Nakagawa, H. Kamada, S. Tsunoda, Y. Tsutsumi, The augmentation of intracellular delivery of peptide therapeutics by artificial protein transduction domains, Biomaterials 30 (2009) 3318–3323.
[10] G.G. Prive, A. Melnick, Specific peptides for the therapeutic targeting of oncogenes, Curr. Opin. Genet. Dev. 16 (2006) 71–77.
[11] S. Racanicchi, C. Maccherani, C. Liberatore, M. Billi, V. Gelmetti, M. Panigada, G. Rizzo, C. Nervi, F. Grignani, Targeting fusion protein/corepressor contact restores differentiation response in leukemia cells, EMBO J. 24 (2005) 1232–1242.
[12] A. Toro, M. Paiva, C. Ackerley, E. Grunebaum, Intracellular delivery of purine nucleoside phosphorylase (PNP) fused to protein transduction domain corrects PNP deficiency in vitro, Cell. Immunol. 240 (2006) 107–115.
[13] A. Toro, E. Grunebaum, TAT-mediated intracellular delivery of purine nucleoside phosphorylase corrects its deficiency in mice, J. Clin. Invest. 116 (2006) 2717–2726.
[14] H.Y. Yoon, S.H. Lee, S.W. Cho, J.E. Lee, C.S. Yoon, J. Park, T.U. Kim, S.Y. Choi, TAT-mediated delivery of human glutamate dehydrogenase into PC12 cells, Neurochem. Int. 41 (2002) 37–42.
[15] E.S. Kim, S.W. Yang, D.K. Hong, W.T. Kim, H.G. Kim, S.K. Lee, Cell-penetrating DNA-binding protein as a safe and efficient naked DNA delivery carrier in vitro and in vivo, Biochem. Biophys. Res. Commun. 392 (2010) 9–15.
[16] J.M. Choi, M.H. Ahn, W.J. Chae, Y.G. Jung, J.C. Park, H.M. Song, Y.E. Kim, J.A. Shin, C.S. Park, J.W. Park, T.K. Park, J.H. Lee, B.F. Seo, K.D. Kim, E.S. Kim, D.H. Lee, S.K.

Lee, Intranasal delivery of the cytoplasmic domain of CTLA-4 using a novel protein transduction domain prevents allergic inflammation, Nat. Med. 12 (2006) 574–579.

[17] J. El-Benna, P.M. Dang, M.A. Gougerot-Pocidalo, Priming of the neutrophil NADPH oxidase activation: role of p47^{phox} phosphorylation and NOX2 mobilization to the plasma membrane, Semin. Immunopathol. 30 (2008) 279–289.

[18] J.D. Lambeth, NOX enzymes and the biology of reactive oxygen, Nat. Rev. Immunol. 4 (2004) 181–189.

[19] A.D. Kennedy, F.R. DeLeo, Neutrophil apoptosis and the resolution of infection, Immunol. Res. 43 (2009) 25–61.

[20] W.M. Nauseef, How human neutrophils kill and degrade microbes: an integrated view, Immunol. Rev. 219 (2007) 88–102.

[21] P.M. Dang, A. Stensballe, T. Boussetta, H. Raad, C. Dewas, Y. Kroviarski, G. Hayem, O.N. Jensen, M.A. Gougerot-Pocidalo, J. El-Benna, A specific p47^{phox}-serine phosphorylated by convergent MAPKs mediates neutrophil NADPH oxidase priming at inflammatory sites, J. Clin. Invest. 116 (2006) 2033–2043.

[22] K.D. Martyn, M.J. Kim, M.T. Quinn, M.C. Dinauer, U.G. Knaus, p21-activated kinase (Pak) regulates NADPH oxidase activation in human neutrophils, Blood 106 (2005) 3962–3969.

[23] B. Polack, S. Vergnaud, M.H. Paclet, D. Lamotte, B. Toussaint, F. Morel, Protein delivery by Pseudomonas type III secretion system: ex vivo complementation of p67(phox)-deficient chronic granulomatous disease, Biochem. Biophys. Res. Commun. 275 (2000) 854–858.

[24] N. Takahashi, K. Matsumoto, H. Saito, T. Nanki, N. Miyasaka, T. Kobata, M. Azuma, S.K. Lee, S. Mizutani, T. Morio, Impaired CD4 and CD8 effector function and decreased memory T cell populations in ICOS-deficient patients, J. Immunol. 182 (2009) 5515–5527.

[25] T. Morio, S.H. Hanissian, L.B. Bacharier, H. Teraoka, S. Nonoyama, M. Seki, J. Kondo, H. Nakano, S.K. Lee, R.S. Geha, J. Yata, Ku in the cytoplasm associates with CD40 in human B cells and translocates into the nucleus following incubation with IL-4 and anti-CD40 mAb, Immunity 11 (1999) 339–348.

Overexpression of T-bet Gene Regulates Murine Autoimmune Arthritis

Yuya Kondo,[1] Mana Iizuka,[1] Ei Wakamatsu,[2] Zhaojin Yao,[1] Masahiro Tahara,[1] Hiroto Tsuboi,[1] Makoto Sugihara,[1] Taichi Hayashi,[1] Keigyou Yoh,[1] Satoru Takahashi,[1] Isao Matsumoto,[1] and Takayuki Sumida[1]

Objective. To clarify the role of T-bet in the pathogenesis of collagen-induced arthritis (CIA).

Methods. T-bet–transgenic (Tg) mice under the control of the CD2 promoter were generated. CIA was induced in T-bet–Tg mice and wild-type C57BL/6 (B6) mice. Levels of type II collagen (CII)–reactive T-bet and retinoic acid receptor–related orphan nuclear receptor γt (RORγt) messenger RNA expression were analyzed by real-time polymerase chain reaction. Criss-cross experiments using CD4+ T cells from B6 and T-bet–Tg mice, as well as CD11c+ splenic dendritic cells (DCs) from B6 and T-bet–Tg mice with CII were performed, and interleukin-17 (IL-17) and interferon-γ (IFNγ) in the supernatants were measured by enzyme-linked immunosorbent assay. CD4+ T cells from B6, T-bet–Tg, or T-bet–Tg/IFNγ$^{-/-}$ mice were cultured for Th17 cell differentiation, then the proportions of cells producing IFNγ and IL-17 were analyzed by fluorescence-activated cell sorting.

Results. Unlike the B6 mice, the T-bet–Tg mice did not develop CIA. T-bet–Tg mice showed overexpression of *Tbx21* and down-regulation of *Rorc* in CII-reactive T cells. Criss-cross experiments with CD4+ T cells and splenic DCs showed a significant reduction in IL-17 production by CII-reactive CD4+ T cells in T-bet–Tg mice, even upon coculture with DCs from B6 mice, indicating dysfunction of IL-17–producing CD4+ T cells. Inhibition of Th17 cell differentiation under an in vitro condition favoring Th17 cell differentiation was observed in both T-bet–Tg mice and T-bet–Tg/IFNγ$^{-/-}$ mice.

Conclusion. Overexpression of T-bet in T cells suppressed the development of autoimmune arthritis. The regulatory mechanism of arthritis might involve dysfunction of CII-reactive Th17 cell differentiation by overexpression of T-bet via IFNγ-independent pathways.

Rheumatoid arthritis (RA) is a chronic inflammatory disorder characterized by autoimmunity, infiltration of the joint synovium by activated inflammatory cells, and progressive destruction of cartilage and bone. Although the exact cause of RA is not clear, T cells seem to play a crucial role in the initiation and perpetuation of the chronic inflammation in RA.

The Th1 cell subset has long been considered to play a predominant role in inflammatory arthritis, because T cell clones from RA synovium were found to produce large amounts of interferon-γ (IFNγ) (1). Recently, interleukin-17 (IL-17)–producing Th17 cells have been identified, and this newly discovered T cell population appears to play a critical role in the development of various forms of autoimmune arthritis in experimental animals, such as those with glucose-6-phosphate isomerase–induced arthritis (2) and collagen-induced arthritis (CIA) (3). Conversely, IFNγ has antiinflammatory effects on the development of experimental arthritis (4,5). IL-17 is spontaneously produced by RA synovium (6), and the percentage of IL-17–positive CD4+ T cells